BIOMARKERS, VOL. 8, NOS. 3–4 (MAY–AUGUST 2003), 240–271

Potential urinary and plasma biomarkers of peroxisome proliferation in the rat: identification of *N*-methylnicotinamide and *N*-methyl-4-pyridone-3-carboxamide by ^{1}H nuclear magnetic resonance and high performance liquid chromatography

STEPHANIE RINGEISSEN[1], SUSAN C. CONNOR[1], H. ROGER BROWN[2], BRIAN C. SWEATMAN[1], MARK P. HODSON[1], STEVE P. KENNY[1], RICHARD I. HAWORTH[1], PAUL MCGILL[1], MARK A. PRICE[1], MIKE C. AYLOTT[3], DEREK J. NUNEZ[4], JOHN N. HASELDEN[1] and CATHERINE J. WATERFIELD[1]*

[1] Safety Assessment, GlaxoSmithKline, Park Road, Ware, Herts, SG12 ODP, UK
[2] Safety Assessment, GlaxoSmithKline, Five Moore Drive, PO Box 13398, Research Triangle Park, North Carolina 27709, USA
[3] Statistical and Data Sciences, GlaxoSmithKline, Park Road, Ware, Herts, SG12 ODP, UK
[4] Discovery Medicine – Metabolic Diseases, GlaxoSmithKline, Five Moore Drive, PO Box 13398, Research Triangle Park, North Carolina 27709, USA

Received 7 March 2003, revised form accepted 7 May 2003

This study identified two potential novel biomarkers of peroxisome proliferation in the rat. Three peroxisome proliferator-activated receptor (PPAR) ligands, chosen for their high selectivity towards the PPARα, -δ and -γ subtypes, were given to rats twice daily for 7 days at doses known to cause a pharmacological effect or peroxisome proliferation. Fenofibrate was used as a positive control. Daily treatment with the PPARα and -δ agonists produced peroxisome proliferation and liver hypertrophy. ^{1}H nuclear magnetic resonance spectroscopy and multivariate statistical data analysis of urinary spectra from animals given the PPARα and -δ agonists identified two new potential biomarkers of peroxisome proliferation – *N*-methylnicotinamide (NMN) and *N*-methyl-4-pyridone-3-carboxamide (4PY) – both endproducts of the tryptophan-nicotinamide adenine dinucleotide (NAD^+) pathway. After 7 days, excretion of NMN and 4PY increased 24- and three-fold, respectively, following high doses of fenofibrate. The correlation between total NMN excretion over 7 days and the peroxisome count was $r = 0.87$ ($r^2 = 0.76$). Plasma NMN, measured using a sensitive high performance liquid chromatography method, was increased up to 61-fold after 7 days' treatment with high doses of fenofibrate. Hepatic gene expression of aminocarboxymuconate-semialdehyde decarboxylase (EC 4.1.1.45) was downregulated following treatment with the PPARα and -δ agonists. The decrease was up to 11-fold compared with controls in the groups treated with high doses of fenofibrate. This supports the link between increased NMN and 4PY excretion and regulation of the tryptophan-NAD^+ pathway in the liver. In conclusion, NMN, and possibly other metabolites in the pathway, are potential non-invasive surrogate biomarkers of peroxisome proliferation in the rat.

Keywords: biomarkers, *N*-methylnicotinamide, *N*-methyl-4-pyridone-3-carboxamide, biofluid nuclear magnetic resonance spectroscopy, metabonomics, multivariate data analysis, rat plasma, rat urine, peroxisome proliferator-activated receptor, peroxisome

* Corresponding author. Catherine J. Waterfield, Safety Assessment, GlaxoSmithKline, Park Road, Ware, Herts, SG12 ODP, UK. Tel: (+44) 1920882679; fax: (+44) 1920882601; e-mail: Cathy.J.Waterfield@gsk.com

Biomarkers ISSN 1354-750X print/ISSN 1366-5804 online © 2003 Taylor & Francis Ltd
http://www.tandf.co.uk/journals
DOI: 10.1080/1354750031000149124

proliferation, aminocarboxymuconate-semialdehyde decarboxylase, quinolinate phosphoribosyltransferase, mRNA levels, tryptophan-nicotinamide adenine dinucleotide pathway.

Introduction

A number of hypolipidaemic drugs used to treat hypertriglyceridaemia and mixed hyperlipidaemia cause peroxisome proliferation in rodents and have been classed as non-genotoxic carcinogens. Peroxisome proliferation in rats and mice is characterized by a marked increase in the size and number of liver peroxisomes. These organelles are responsible for β-oxidation of long-chain fatty acids and are involved in cholesterol metabolism. In addition, peroxisome proliferators cause liver hypertrophy and hyperplasia in rodents, leading to the growth of hepatocellular carcinomas. Both the peroxisome proliferation response and the lipid-modulating effects of these compounds appear to be mediated through the peroxisome proliferator-activated receptor α (PPARα). This is a member of the nuclear hormone receptor superfamily, known to induce changes in the transcription of genes encoding enzymes involved in lipid and lipoprotein metabolism. Recent investigations with a potent and selective PPARδ agonist have shown that the peroxisome proliferation caused by administration of high doses of the PPARδ resulted from activation of PPARα (Romach *et al*. 2002) rather than stimulation of the PPARδ receptor. Although the correlation of peroxisome proliferation with hepatocarcinogenesis is compelling, the generic mechanism by which this class of chemicals induces liver tumours is still not understood. Recent findings suggest that peroxisome proliferators could activate growth regulatory pathways, largely via PPARα-independent mechanisms (Pauley *et al*. 2002).

Long-term treatment of primates with fibrates such as ciprofibrate, clobuzarit or clofibrate does not result in an increase in hepatocellular carcinoma. However, peroxisome proliferation has been reported to be induced in some non-human primates (rhesus and cynomolgus monkeys) (Reddy *et al.* 1984, Lalwani *et al*. 1985). Although there have been no reports of increased incidence of hepatic carcinoma, these studies were not of lifetime duration, and other data is limited (Reddy *et al*. 1984, Ashby *et al*. 1994, Lake 1995a,b, Tucker and Orton 1995).

Although human and non-human primates are generally believed to be refractory to peroxisome proliferation, this has not been adequately evaluated at clinically relevant exposures in primates. Recent data in male cynomolgus monkeys has shown that peroxisome counts increased up to 2.7-fold when treated with clinically relevant doses (up to four times greater than the clinical exposure) of fenofibrate and ciprofibrate for 15 days (Qualls *et al*. 2003). The same animals had significant two-fold increases in liver weight, hepatocyte hypertrophy, and more than a two-fold increase in mitochondrial numbers. Mitochondrial but not peroxisomal area was increased. However, there was no evidence of cell cycle alterations or DNA damage, and only equivocal evidence of oxidative stress at the cytological or transcriptomic level.

There is little, if any, evidence for significant peroxisome proliferation in human liver (Ashby *et al*. 1994). Long-term treatment (3–94 months) of hypertriglyceridaemia patients with ciprofibrate resulted in limited peroxisome proliferation, with

significant increases in the number of peroxisomes but not in their volume density observed during the first months of treatment (Hanefeld *et al*. 1983). In another study, fibrate administration to humans at pharmacological doses did not increase the hepatic expression of acyl-coenzyme A (CoA) oxidase, a marker of peroxisome proliferation in rodents (Roglans *et al*. 2002). In addition, human hepatocytes appear to be resistant to chemically induced peroxisome proliferation (Moody *et al*. 1991, Bentley *et al*. 1993, Ashby *et al*. 1994, IARC 1995, Lake 1995b, Elcombe *et al*. 1997).

Assessment of human hepatic responses to PPARα agonists is hampered by the lack of biomarkers of peroxisome proliferation and of a complete understanding of the mechanism of hepatic effects in rodents. We have been investigating an alternative approach to the problem of monitoring peroxisome proliferation. This is usually assessed in tissue samples taken by biopsy or at necropsy. Current techniques to characterize peroxisome proliferation include transmission electron microscopy to identify peroxisomes, identification of peroxisomal catalase, urate oxidase and acyl-CoA oxidase by measuring enzyme activity or the protein by immunohistochemistry. However, these are invasive, time-consuming techniques, and not amenable to continuous monitoring. An alternative approach to monitoring adverse drug reactions/pathologies is to identify urinary or plasma biomarkers that may be surrogates and/or have a direct correlation with the pathology. One way to identify such novel biomarkers is to use an open system such as analysis of urine and plasma using high frequency ^{1}H nuclear magnetic resonance (^{1}H NMR) spectroscopy. The spectra generated contain data on potentially hundreds of endogenous metabolites, providing information on patterns of excretion of endogenous metabolites or single molecules. If samples are collected continuously, temporal information on the metabolites can be obtained. Since the spectra contain thousands of resonances, statistical data reduction and multivariate statistical data analysis (MVDA), such as principal components analysis, are used. This helps to determine what resonances cause separation of the data, and which components are correlated with each other. This NMR MVDA approach is described as 'metabonomics' (Nicholson *et al*. 1999). ^{1}H NMR has been used to successfully identify other putative biomarkers such as phenylacetylglycine (phospholipidosis) (Nicholls *et al.* 2000), taurine (liver dysfunction) (Sanins *et al*. 1990) and creatine (testicular injury) (Nicholson *et al*. 1989), allowing the condition to then be investigated by more conventional biochemical means.

Metabonomics was used in the present study to identify biomarkers of peroxisome proliferation in the urine of rats treated with fenofibrate and three compounds produced by GlaxoSmithKline with activity almost exclusively at the PPARα, -δ or -γ subtypes. PPARα and -δ agonists have lipid-lowering pharmacological properties (reduced plasma triglycerides and increased high density lipoproteins), while the γ agonist class of compounds increase insulin sensitivity and are indicated in type II diabetes.

This study was designed to generate a variety of data, including clinical chemistry, limited pathology and clinical observations, transmission electron microscopy, immunohistochemistry (IHC) for catalase, ^{1}H NMR of urine and plasma, high performance liquid chromatography (HPLC) analysis of plasma, and

gene expression in liver. The aim was to identify cellular changes or pharmacologically related changes in the endogenous metabolism of rats treated with PPAR ligands that might correlate with the extent of peroxisome proliferation. Due to the short duration of this study, it was not anticipated that any biomarker of hepatocarcinogenesis would be identified in addition to markers of peroxisome proliferation, as there would be no suitable endpoint with which to correlate the NMR findings. Biochemical changes in plasma and urine, as well as altered gene expression in the liver, were investigated for their potential to be used as biomarkers of peroxisome proliferation.

Materials and methods

Chemicals and reagents

N-Methylnicotinamide chloride salt (NMN) was purchased from Sigma-Aldrich (Gillingham, Dorset, UK). *N*-methyl-2-pyridone-3-carboxamide (2PY), *N*-methyl-4-pyridone-3-carboxamide (4PY) and *N*-ethylnicotinamide (NEN) were synthesized according to the method outlined by Bernofsky (1979). The purity of the solids obtained was estimated to be $>99\%$.

Animals and treatments

Male Wistar Han rats (65–72 days old on day 0, weight 256–312 g) were obtained from Charles River UK Ltd (Margate, UK). Animals were randomly allocated into nine groups ($n = 5$ per group) and were housed five per cage in Techniplast animal cages (type 4) for 9 days following arrival. They were then acclimatized in grid-bottomed urine collection cages (MET 1,20 metabolism cage, Arrowmight-Biosciences, Hereford, UK) for three 8 h periods during the day, prior to continuous housing in such cages for 7 days to allow for the continuous collection of urine throughout the study. Throughout the acclimatization and study periods, rats had access to food (Rat and Mouse 1, SDS, Manea, UK) and water *ad libitum*. They were maintained on a 12 h light/dark cycle with the lights programmed to be changed at 8 a.m. and 8 p.m. to coincide with the change in urine collection and morning dosing period. The room was maintained at 19–23°C at a humidity of 45–70%.

Three PPAR agonists used as research tools, GWα, GWδ and GWγ, with a high degree of selectivity for the PPARα, δ and γ receptors, respectively (Table 1), and fenofibrate (predominantly α) were provided by research chemistry laboratories within GlaxoSmithKline Research and Development. Two dose levels were selected for each compound. The low dose was to provide similar pharmacological effects (e.g. lipid lowering) and the high dose was set 10-fold higher in order to cause peroxisome proliferation in the case of the PPARα ligands. The PPARγ agonist was not expected to cause peroxisome proliferation. Fenofibrate was used as a positive control at a dose that produces the therapeutic effects of lipid lowering as well as the secondary effects such as liver enlargement and peroxisome proliferation.

Each group of animals were given an oral dose by gavage twice daily for 7 consecutive days, at 8 a.m. and 4 p.m., of GWα, GWδ, GWγ, fenofibrate (0.5% w/w hydroxypropylmethylcellulose and 0.1% w/w Polysorbate 80 in phosphate buffer, pH 7, 2 ml kg^{-1}) or vehicle control. The first day of dosing was day 0, and all animals were killed on day 7. Body weights were recorded once daily from day −3 through to day 7. All treatments were carried out under the appropriate Home Office licence.

Table 1. Activity of PPARs agonists in cell-based transactivation assays.

	Murine receptor EC_{50} (μM)		
Compound	PPARα	PPARδ	PPARγ
Fenofibrate	18	i.a. at 100	250
GWα	0.005	i.a.	2.2
GWδ	8.9	0.028	i.a.
GWγ	i.a.	i.a.	0.0012

All data was generated using the PPAR-GAL4 transactivation assay using an SPAP reporter as described in Henke *et al.* (1998).

Values are $\pm 20\%$, $n \geq 3$.

i.a., inactive at 10 μM or the concentration indicated, EC_{50}, effective concentration 50% level.

Sample collection

Urine was collected from all animals for 8 h during each of the 3 days of the acclimatization period to the urine collection cages, and then continuously between 8 a.m. and 4 p.m., 4 p.m. and 12 a.m., and 12 a.m. and 8 a.m. for the 7 day treatment period. All collections were timed to start after dosing (carried out at 8 a.m. and 4 p.m.) and were collected into 1% sodium azide (1 ml), which acted as a bacteriocide. Urine volumes were recorded and the samples retained at −80°C until analysis by ^{1}H NMR spectroscopy.

On day 7, animals were killed by exsanguination under isoflurane anaesthesia. Blood samples were collected via the aorta into heparinized containers for ^{1}H NMR spectroscopic analysis and into Microtainers® for assessment of clinical chemistry by HPLC and measurement of clinical pathology parameters. For ^{1}H NMR spectroscopy, plasma samples were prepared by centrifugation (15 min at 1500 *g* at 20°C), and aliquots stored at −80°C until analysis. Remaining blood samples were analysed by routine methodologies (Hitachi 917 random discrete analyser) for assessment of plasma clinical chemistry parameters, including aspartate aminotransferase (AST), alanine aminotransferase (ALT), alkaline phosphatase (ALP), cholesterol, glucose, total protein, albumin, high density lipoprotein (HDL), low density lipoprotein (LDL), very low density lipoprotein (VLDL) and triglyceride (TRG).

Known target organs were removed at autopsy, including liver, kidney, thyroid and adipose tissue. Samples were fixed in 10% w/v phosphate buffered formalin and embedded in paraffin wax. Sections (4 μm) were cut and stained with Mayer's haematoxylin and eosin for light microscopy. Some liver samples were 'snap-frozen' in liquid nitrogen for subsequent analysis of mRNA expression of specific enzymes.

Transmission electron microscopy for peroxisome numbers and distribution

Livers from two animals (chosen at random) from each group were examined. Pieces of liver (2 mm^3) were selected from the residual formalin-fixed material and washed overnight in 0.1 M cacodylate buffer. A combination of 1.5% w/v potassium ferrocyanide/1% w/v osmium tetroxide in 0.1 M cacodylate buffer was then used for secondary fixation prior to dehydration in ascending concentrations of ethanol and dried acetone and processing into Spurr's resin. Ultra-thin sections (90 nm) of a centrilobular and a periportal area from each animal were prepared, stained with uranyl acetate and lead citrate, and examined using a Philips CM10 transmission electron microscope. Only the cells within the first six closest to a central vein or bile duct were examined. This was to ensure that mid-zonal cells were not mistakenly examined. Also, for each cell assessed, it was ensured that the nucleus and cell boundary were completely unobscured by grid bars.

For each animal the number of peroxisomes in 10 cells from both a periportal and a centrilobular area were counted, that is a total of 20 cells per animal. The mean number of periportal and centrilobular peroxisomes per cell for each animal, and the mean number of peroxisomes per cell for each treatment (% control) were calculated.

Catalase IHC on fixed liver tissue

IHC staining for catalase is a well-characterized method for evaluating peroxisome proliferation (Hollinshead and Meijer, 1988). Livers from two animals per group (the same animals used for the peroxisome counts) were examined. Paraffin wax-embedded tissues were sectioned at 3–7 μm and immunostained with a rabbit polyclonal antibody to catalase (Chemicon AB1212). Adjacent sections of liver were immunostained with a rabbit polyclonal antibody to thyroglobulin (Dako A251) at matched concentrations (1:1000) to provide a negative control. Three separate IHC analyses were carried out.

^{1}H NMR analysis of urine

Sample preparation. Aliquots of urine (400 μl) were mixed with phosphate buffer (200 μl, 0.2 M, pH 7.4) and left to stand at room temperature for 10 min. Any resulting precipitate was removed by centrifugation at 5000 r.p.m. for 15 min at 4°C. From the supernatant, an aliquot (500 μl) was put into a 5 mm NMR tube (Wilmad 507PP) to which an aliquot (50 μl) of a sodium 3-trimethylsilyl-(2,2,3,3-$^2H_4$)-1-propionate (TSP)/D_2O/sodium azide solution (0.1% w/v TSP in D_2O and 1% w/v sodium azide) had been previously added.

^{1}H NMR analysis. The TSP and D_2O provided a chemical shift reference ($\delta_H = 0.00$ p.p.m.) and deuterium lock signal for the NMR spectrometer. Samples were analysed at 600.13 MHz on a Bruker DRX-600 spectrometer at ambient probe temperature (300 K) using a 5 mm TXI ATMA probe.

Spectra were acquired using a standard presaturation pulse sequence for water suppression incorporating the first increment of the NOESY:

$$RD - 90^\circ - t_1 - 90^\circ - t_m - 90^\circ - \text{collect FID}$$

where RD was a relaxation delay of 2 s, during which the water was selectively irradiated, FID was the free induction decay, t_1 represented the first increment in a NOESY experiment and was set to 3 μs, and t_m had a value of 100 ms, during which the water resonance was again selectively irradiated. A total of 64 scans and four dummy scans were collected into 64k computer data points, with a spectral width of 12019.23 Hz an acquisition time of 2.73 s and a relaxation delay of 2.00 s (total recycle delay of 4.73 s). The FIDs from each sample were multiplied by an exponential line-broadening function of 0.30 Hz prior to Fourier transformation (FT).

Two-dimensional (2D) NMR spectra were acquired on selected samples to enable identification of the potential biomarkers. 2D ^{1}H-^{1}H total correlation spectroscopy (TOCSY) NMR spectra were acquired using 32 scans collected into 2k data points per increment for 256 increments, with F1 and F2 spectral widths of 10.2 p.p.m. The FIDs were multiplied by a shifted sine-bell squared function in both dimensions prior to FT. Heteronuclear multiple bond correlation (HMBC) ^{1}H-^{13}C spectra were acquired for selected samples using 4k data points in F2 with 256 increments and 384 scans per experiment. Solvent suppression was carried out during 0.5 s relaxation delay. The F2 spectral width was 13.3 p.p.m. and the F1 spectral width was 239 p.p.m. The FIDs were weighted using a sine-bell squared function in both dimensions prior to FT.

Heteronuclear single quantum coherence (HSQC) ^{1}H-^{13}C spectra were acquired for selected samples using 4k data points in F2 with 512 increments and 256 scans per experiment. The F2 spectral width was 13.3 p.p.m. and the F1 spectral width was 180 p.p.m. The FIDs were weighted using a sine-bell squared function in both dimensions prior to FT.

MVDA of NMR spectral data from urine samples. All spectra were phased and baseline corrected using XWINNMR (Bruker GmbH, Karlsruhe, Germany). Data were reduced to 245 integrated regions (buckets) of 0.04 p.p.m. corresponding to the region δ10.0–0.2 p.p.m. using AMIX (Bruker GmbH). The region δ6.0–4.5 p.p.m. was excluded from MVDA because of the high variability in the intensity of the water and urea resonances during the NOESYPR1D experiment. Before the resulting integral regions were imported into SIMCA-P (V8.0, Umetrics AB) to carry out MVDA, the NMR data were normalized to the total area of each spectrum. Data were then mean centred and scaled either to unit variance by dividing through by the standard deviation of the variable or using Pareto scaling to set the variation to the original standard deviation of the variable prior to scaling. Principal components analysis and partial least squares discriminant analysis were then carried out to look for patterns in the data.

Calculation of urinary concentrations and amounts excreted of NMN and 4PY using NMR spectral data from urine. Concentrations (μM) of NMN and 4PY were estimated in the urine of control and treated animals using ^{1}H NMR spectra (internal reference: TSP at a concentration of 527 μM in the NMR tube) and peak areas calculated by the AMIX software, over the three 8 h collection periods of each day (from day −1 to day 6). The formulae used were:

$$C_{NMN} = (A_{NMN} \times C_{TSP}/A_{TSP}) \times (N/n) \times CD$$

$$C_{4PY} = (A_{4PY} \times C_{TSP}/A_{TSP}) \times (N/n) \times CD$$

where A_{NMN} is the area of the NMN peak on the NMR spectrum (bucket 9.26), A_{4PY} is the area of the 4PY peak on the NMR spectrum (bucket 8.54), A_{TSP} is the area of the TSP peak on the NMR spectrum (buckets −0.02 and +0.02), C_{NMN} is the concentration of NMN in the non-diluted urine sample (μM), C_{4PY} is the concentration of 4PY in the non-diluted urine sample (μM), C_{TSP} is the concentration of TSP in the NMR tube (527 μM), N is the number of protons included in the TSP peak ($N = 9$), n is the number of protons included in the NMN or 4PY peaks ($n = 1$), and CD is the coefficient of dilution of urine in the final NMR sample (CD = 1.65).

Using the volume of urine measured for each of the three periods, the amount of NMN and 4PY excreted by each animal during these times was calculated (μmol per 8 h). The total amount excreted per 24 h was then deduced by summing the amounts excreted over the three 8 h periods (μmol per 24 h). Absolute amounts were finally expressed per body weight unit (μmol kg^{-1} per 8 or 24 h).

^{1}H NMR analysis of plasma

Sample preparation. Plasma samples were defrosted at ambient temperature. D_2O (200 μl) was added to the aliquots (500 μl). Following centrifugation (20 min at 2400 *g* at 4°C), the supernatants were transferred into 5 mm Wilmad 507 PP NMR tubes. The tubes were inverted several times to ensure thorough mixing.

^{1}H NMR analysis. ^{1}H chemical shifts were referenced internally to the α-glucose ^{1}H resonance at δ5.236, previously measured relative to the primary internal chemical shift reference TSP at δ0.00. Samples were analysed at 600.13 MHz on a Bruker DRX-600 spectrometer at ambient probe temperature (300 K) using a 5 mm TXI ^{1}H probe. In order to suppress the large water signal, spectra were acquired with the pulse sequence NOESYPR1D already mentioned for the ^{1}H NMR analysis of urine and a total of 128 scans.

Spectra were also acquired using a Carr-Purcell-Meiboom-Gill (CPMG) spin-echo experiment (with presaturation of the water resonance) using the following pulse sequence:

$$\mathrm{RD} - 90^\circ_x(\tau - 180^\circ_y - \tau)_n - 90^\circ - t_m - \text{collect FID}$$

with 128 scans and four dummy scans into 64k computer data points, a spectral width of 12019.23 Hz, an acquisition time of 2.73 s and a relaxation delay of 2.00 s (total delay between pulse cycles of 4.73 s). The fixed delay τ, set at 830 μs, allows spectral editing via faster T2 relaxation and hence attenuation of broad signals. The total spin–spin relaxation delay ($2n\tau$) was 212.5 ms. The FIDs from each sample were multiplied by an exponential line-broadening function of 0.30–0.50 Hz prior to FT for all experiments.

HPLC spectrofluorimetric analysis of plasma samples

Following ^{1}H NMR urinalysis, many metabolites of interest were identified as changing in response to PPAR drug treatment. One of these, NMN, was selected for quantification by HPLC. A method recently developed for the determination of urinary and plasma levels of NMN was used (Musfeld *et al*. 2001), with a few modifications as detailed below. The chromatographic system consisted of a 1050 series pump (Hewlett-Packard, Waldbrown, Germany) connected to an autosampler and a 474 scanning fluorescence detector (Waters, Milford, USA). Chromatographic separations were performed using a C18-MN5-23057 (250 × 3.2 mm internal diameter) column (Capital HPLC Ltd, Leeds, UK) equipped with a C18 security guard cartridge (4 × 2 mm internal diameter) (Phenomenex, Macclesfield, UK). The flow rate was set to 0.75 ml min^{-1}.

The volume of plasma samples to be used for the derivatization procedure in the original paper was reduced to 100 μl (all volumes of other solutions used for the preparation were also divided by a factor of 2) so that samples could be prepared and run in duplicate.

The use of water in place of plasma for the preparation of standard curves was shown to be acceptable, as the curves prepared using water and plasma had equivalent gradients (i.e. were parallel) and the intercept for the water curve, containing no endogenous NMN, passed close to zero. Calibration curves were linear (r^2 always > 0.999) up to 1000 ng ml^{-1} (7.3 μM). NMN was shown not to be lost through protein binding (data not shown).

The retention times of NMN and NEN (as internal standard) were 6.4 and 8.2 min, respectively, with a total run time of 18 min. Results are the mean of duplicate samples.

Levels of mRNA for QAPRT and ACMSD

Two key enzymes in the metabolic pathway of interest were identified in literature searches as being altered by PPARα and -δ ligands. These enzymes, aminocarboxymuconate-semialdehyde decarboxylase (ACMSD, EC 4.1.1.45) and quinolinate phosphoribosyltransferase (QAPRT, EC 2.4.2.19), were selected for further RNA quantification.

Total RNA extraction. Total RNA was extracted from liver tissues using the SV RNA Isolation Kit according to the manufacturer's instructions (Promega UK Ltd). RNA integrity was assessed using an Agilent 2100 Bioanalyser.

cDNA synthesis. Total RNA (2 μg) was reverse transcribed using the SuperScript™ First Strand Synthesis System for reverse transcription-polymerase chain reaction (RT-PCR) (Invitrogen) in a total reaction volume of 20 μl. The reactions were carried out according to the manufacturer's instructions using a thermal cycler (Tetrad DNA Engine, MWG-Biotech Ltd). Samples were then made up to 100 μl with RNAse/DNAse-free water. Reactions were carried out in triplicate for each animal. An additional fourth reaction was included in which the reverse transcriptase was omitted to serve as a negative control to confirm the absence of genomic DNA contamination.

TaqMan® probes and primers. PCR primers and TaqMan® probes specific for the target sequences (Table 2) were designed using the Primer Express software package (Applied Biosystems).

The DNA sequence of rat (*Rattus norvegicus*) ACMSD was obtained from GenBank (accession no. AB069781). The PCR primers and TaqMan® probes were commercially synthesized by MWG-Biotech

Table 2. Sequences of PCR primers and TaqMan® probes for ACMSD and QAPRT target sequences.

ACMSD (accession no. AB069781)	
Forward primer	5′ GCT GGC TGT CGA GGA GAT G 3′
Reverse primer	5′ TGA TGT GGG ATC CAA TCT GGA T 3′
TaqMan® probe (FAM-labelled)	5′ CCT GGA AAT CCT AGC TCC TTT ACA CAA CGC T 3′
QAPRT (accession no. BI282155 for the EST used)	
Forward primer	5′ AGA ATG GAT TAC TGT GGC TTG TTG 3′
Reverse primer	5′ GTG GGA AGC CTA GGT AAA TTT CAG 3′
TaqMan® probe (FAM-labelled)	5′ CAC ACA TCT TTA GGT TCA GAG GCC AAC A 3′

FAM, 6-carboxyfluorescein, a fluorescent tag.

Ltd (Milton Keynes, UK) and Applied Biosystems, respectively. At the time of the study, the sequence for rat QAPRT was not available in the public domain. However, a number of expressed sequence tags (ESTs) were available for the rat that revealed a very high sequence homology with both human and murine QAPRT transcripts (80% and 91% sequence homology, respectively). A single representative EST was selected for use in this study (accession no. BI282155). It should be noted that the sequence under this accession number is non-coding; therefore it was inverted and reverse complemented prior to comparison with the human QAPRT (accession no. D78177) and murine (accession no. AK010602) QAPRT transcripts.

Real-time quantitative PCR. Real-time PCR was carried out using an ABI 7900 sequence detection system (Applied Biosystems). The expression level of 18S ribosomal RNA was determined to allow normalization of the gene expression data. Samples were added to a 96-well TaqMan® MicroAmp Optical Plate and placed into the 7900 sequence detection system. Thermal cycling was initiated with incubation at 50°C for 2 min and at 95°C for 10 min. After this initial step, a further 40 PCR cycles of heating at 95°C for 15 s and at 60°C for 1 min were carried out. Rat genomic DNA standards were used from 10^5 to 10^2 copies per well (triplicates) for the ABI7900 software to construct standard curves. Two controls without templates were also included to confirm the absence of nucleic acid contamination.

Statistics

Statistical analysis was performed using Dunnett's test (multiple comparisons against a single control) or a two-way analysis of variance (ANOVA) at levels of significance of 95% or 99% (Dunnett 1955).

Results and discussion

Clinical chemistry and histopathology

None of the doses of GWα, GWδ, GWγ or fenofibrate resulted in reduced food intake or any adverse clinical signs such as weight loss. There was an expected increase in liver weight.

Treatment with GWα, GWδ and fenofibrate resulted in histopathological changes in the liver (periportal hypertrophy and eosinophilia with GWα, centrilobular hypertrophy with GWδ and fenofibrate, and hepatocyte mitotic increase and reduction in glycogen vacuolation with all three) and changes in the thyroid gland (follicular hypertrophy). In addition, treatment with GWδ and fenofibrate resulted in histopathological changes in the kidney (increased incidence of tubular eosinophilic droplets).

The liver changes observed with GWα and fenofibrate are considered to be consistent with peroxisome proliferation, which is associated with the administration of this class of compound to rats (Bybee *et al.* 1990). As a consequence, there was a significant increase in liver weight and plasma ALT activity with the two

PPARα ligands (Table 3). Significant increases in plasma ALP and AST activities were also observed with GWα.

Significant increases in liver weight and plasma ALP activity were observed with the PPARδ agonist. *In vivo* exposure of PPARα-null mice to PPARγ/δ-specific agonists has been previously reported to induce peroxisome proliferation (DeLuca *et al.* 2000). The increase in plasma enzymes was thought to be consistent with liver hypertrophy and is not related to overt cellular damage.

Dose-related reductions in plasma cholesterol, TRG and HDL were seen following treatment with GWα and GWδ, with significant differences from control levels (Table 3). These changes were considered to reflect an alteration in lipid metabolism due to the pharmacological activity of the test material. In addition, reductions in body weight gain and a significant increase in plasma albumin concentration were reported with these two compounds. The same changes were observed in animals treated with fenofibrate, although there was no decrease in plasma LDL in this group.

Treatment with GWγ resulted in histopathological changes in the liver (reduction in glycogen vacuolation) and changes in white and brown adipose tissue, in addition to an increase in body weight gain and a significant reduction in plasma TRG. There was also a decrease in liver weight that may have been due to loss of glycogen. There was an increase in plasma cholesterol, LDL and AST activity in animals given GWγ.

Evidence of peroxisome proliferation

In order to correlate the putative markers identified later in this study with a suitable endpoint for peroxisome proliferation, two endpoints to demonstrate peroxisome proliferation were recorded: peroxisome counts and distribution using transmission electron microscopy on liver sections, and IHC for catalase protein on fixed liver tissue.

Peroxisome counts and distribution using transmission electron microscopy of liver sections. The mean number of peroxisomes per cell for each treatment (expressed as the percentage over control values) was calculated for the periportal and centrilobular areas (Table 4). There was a wide variation between cells of the same treatment group in the number of peroxisomes that they contained, both in the same animal and between the two animals examined per group. The following limits were applied in order to exclude the possibility that differences were only due to sampling variation: an increase greater than 100% above the control values was considered to be due to the treatment; an increase between 50% and 99% was considered to be possibly due to the treatment; and an increase of $< 50\%$ was considered not to be due to the treatment. Within these constraints, peroxisome proliferation was seen with high dose GWα, GWδ and fenofibrate, and possibly with low dose fenofibrate. Low doses of GWα and GWγ did not induce peroxisome proliferation, nor did high doses of GWγ.

There were a greater number of peroxisomes in control cells from the centrilobular area compared with the periportal area. This largely explains why the treatment-related increase in peroxisomes appeared to be greater in the

Table 3. Summary of liver and body weights at autopsy and clinical chemistry parameters showing significant changes after 7 days of repeat dosing.

		GWα		GWδ		GWγ		Fenofibrate	
	Control	LD	HD	LD	HD	LD	HD	LD	HD
Body weight gain from day 0–7 (g)	19.84	22.38	11.74	22.26	16.4	31.42	35.56	23.12	16.02
Liver weight on day 7[a]	10.94 g	+6%	+35%**	+2%	+39%**	−8%	−12%*	+2%	+40%**
Plasma clinical chemistry on day 7									
ALP (IU l^{-1})	328.0	371.4	528.2**	469.4*	454.2*	350.8	324.0	353.4	440.6
ALT (IU l^{-1})	37.10	42.20	47.00**	40.70	33.70	47.30	42.70	34.60	44.10*
AST (IU l^{-1})	53.90	60.70	70.60**	61.40	54.70	74.60*	72.30*	67.00*	69.90*
Albumin (g l^{-1})	38.50	41.22	45.98**	38.62	42.76*	39.04	36.68	41.66	43.12**
Cholesterol (mmol l^{-1})	1.440	1.146*	0.640**	1.334	0.960**	1.518	1.718*	0.808**	0.616**
TRG (mmol l^{-1})	1.698	1.036**	0.686**	1.310*	0.752**	0.428**	0.766**	1.168**	0.828**
HDL (mmol l^{-1})	1.270	0.990*	0.518**	1.198	0.840**	1.328	1.460	0.682**	0.476**
LDL (mmol l^{-1})	0.126	0.116	0.088	0.096	0.070*	0.144	0.208**	0.092	0.106

[a]Percentages are percent of control values.
LD, low dose; HD, high dose; *$p < 0.05$; **$p < 0.01$.

Table 4. Peroxisome count and distribution in liver tissue at autopsy as estimated by transmission electron microscopy. The mean number of peroxisomes per cell (10 cells for each region, $n = 2$ animals per group) was calculated in each area for each group and expressed as a percentage increase with respect to the control values.

Treatment	Dose	Cell region	% increase
GWα	Low	Periportal	29
		Centrilobular	29
	High	Periportal	147
		Centrilobular	117
GWδ	Low	Periportal	65
		Centrilobular	9
	High	Periportal	241
		Centrilobular	145
GWγ	Low	Periportal	18
		Centrilobular	5
	High	Periportal	24
		Centrilobular	5
Fenofibrate	Low	Periportal	88
		Centrilobular	68
	High	Periportal	241
		Centrilobular	200

periportal area. It is, however, uncertain, within the constraints of the methods used, whether the periportal and centrilobular areas differ in their sensitivity to a given peroxisomal proliferator.

IHC for catalase on fixed liver tissue. The different responses of the rat liver to the four different treatments in terms of grade and location of peroxisome proliferation was examined using catalase IHC. This enabled comparison of pathology findings with a more accurate marker of peroxisome proliferation. Previous studies have established the specific localization of catalase in the peroxisomes in rat liver (Hollinshead and Meijer 1988). The use of post-embedding IHC for the detection of catalase is considered an appropriate method for comparing the peroxisome content of tissue (Beier 1992). However, it should be noted that catalase-negative peroxisomes have been demonstrated in the livers of rats following partial hepatectomy (Oikawa and Novikoff 1995) and therefore it is possible that the catalase IHC method used in this study may not have detected the entire population of hepatic peroxisomes.

Treatment-related changes in catalase IHC were observed at autopsy in the liver of animals administered high dose GWα, high dose GWδ and fenofibrate at both dose levels. These changes related to the distribution and/or grade of immunostaining relative to the control group. Treatment with high dose GWα resulted in moderate, portal, catalase-positive granules, which was consistent with the periportal hypertrophy and eosinophilia observed on light microscopy in the liver of all animals treated with a high dose of this PPARα agonist. Treatment with high dose GWδ resulted in slight, irregularly located, catalase-positive granules, indicating that only a minority of hepatocytes within a lobule were responding to the treatment with marked upregulation of catalase. Therefore, the centrilobular hypertrophy and increased liver weight observed in this group do not appear to be

consistent with the IHC findings. No change in catalase staining was observed with GWα or GWδ at low doses. The same observation was made after treatment with GWγ, which is consistent with the lack of liver findings on light microscopy and the absence of weight gain. Treatment with fenofibrate resulted in catalase-positive granules being identified in the centrilobular regions (slight and irregular at low doses, moderate and diffuse at high doses).

Evidence of peroxisome proliferation. Evidence for peroxisome proliferation from transmission electron microscopy and light microscopy, including IHC for catalase, correlated well, although the zonal distribution of peroxisomes cannot be reliably identified by transmission electron microscopy, as limited tissue samples were examined. An increase in peroxisomes was seen by transmission electron microscopy following high doses of GWα, GWδ and fenofibrate (and possibly low doses of fenofibrate), and IHC was positive for catalase protein in the same groups. Thus peroxisome counts determined by transmission electron microscopy were used to correlate with putative biomarkers of peroxisome proliferation.

MVDA of urine NMR data: identification of NMN and 4PY among other potential markers of peroxisome proliferation

Metabonomics has the potential to identify proton-containing endogenous metabolites non-invasively over time, without prior knowledge of the potential changes. The technique was applied to urine and plasma samples in this study. It offers the possibility of identification of endogenous metabolites or patterns of changes, which have the potential to be novel biomarkers of metabolic changes related to toxicity. MVDA of the urinary dataset involved two steps. Initial principal components analysis (PCA) was carried out to enable the major endogenous metabolite changes or any abnormal samples (not representative of the sample population) to be identified rapidly. Then a more in-depth analysis was carried out to reveal more subtle changes in the urinary metabolic profiles.

PCA. Starting with the full dataset minus the predose controls, PCA showed that there were outliers mainly in the GWγ group due to prominent glycosuria, which was thought to be due to altered renal handling of glucose as there was no evidence of renal pathology (Figure 1A). These outliers accounted for the largest source of variation in the data; therefore the decision was taken to remove these samples rather than delete the full sugar region from the dataset.

Subsequent PCA of the dataset minus the outlying samples (Figure 1B) detected further outliers in the dataset due to processing errors and other abnormalities (including bacterial or fungal degradation). A slight clustering of fenofibrate-dosed samples in PC2 was partly due to drug-related resonances. Some signals were assigned to drug-related metabolites following faecal analysis by liquid chromatography/mass spectrometry (data not shown). A singlet at 1.5 p.p.m. seen at both dose levels from day 0 to day 6 in the urine of animals treated with fenofibrate was subsequently excluded from the MVDA. A broad signal at 3.71 p.p.m. present in the first 8 h collections on day 0 in the urine of animals treated

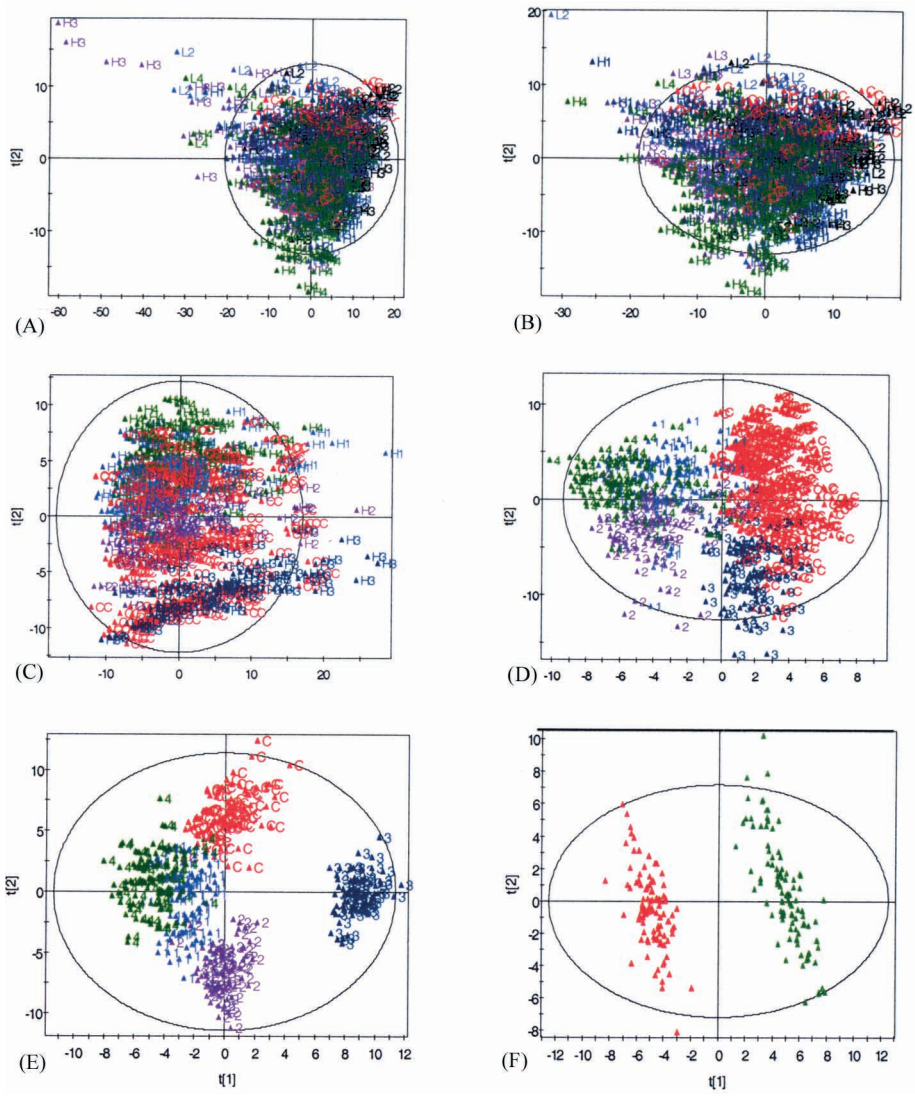

Figure 1. MVDA of the urinary ^{1}H NMR dataset, with PCA and PLS-DA plots illustrating the strategy used. A detailed description of the successive steps is given in the Results and discussion section. For plots A to C: H, high dose; L, low dose; C, control; 1, GWα; 2, GWδ; 3, GWγ; 4, fenofibrate. (A) PCA of the full dataset minus predose controls; (B) PCA of the full dataset minus predose controls and glycosuric samples; (C) PCA of the full dataset minus predose controls and glycosuric samples. Regions of the spectra corresponding to TCA cycle intermediates, hippurate, taurine and drug-related resonances were excluded. For plots D to F: C, control (red); 1, GWα (light blue); 2, GWδ (purple); 3, GWγ (dark blue); 4, fenofibrate (green). (D) PLS-DA of the control and high dose treated groups, minus glycosuric and 0–8 h samples. (E) o-PLS-DA minus 0–48 h samples, orthogonal signal correction. (F) PLS-DA of the control group and the fenofibrate high dose group only.

with high doses of the same compound was also excluded. No drug-related metabolites were detected after treatment with the three other PPAR ligands.

Univariate analysis showed that some of the NMR integral regions were very variable across the dataset, due in part to a shift of some of the metabolite

resonances. An example of this was citrate, which had a highly variable resonance position in the spectrum. It has also been found in the past that levels of certain metabolites change frequently following administration of a wide range of toxins. These included tricarboxylic acid (TCA) cycle intermediates, taurine and hippurate, which may vary with the diet. Subsequent PCA was therefore performed after these regions of the spectra, together with degraded samples, had been deleted.

Analysis of the scores plots from PCA analysis of the reduced dataset showed that there was some separation of the groups in PC2 towards the edges of the control cluster (Figure 1C) and partial separation in some of the lower components. Partial least squares discriminant analysis (PLS-DA) was then carried out on this reduced dataset in order to further resolve the clustering between the dose groups.

PLS-DA. The first PLS-DA (Figure 1D) was carried out using the high dose samples, taking out the glycosuric samples and the 0–8 h samples, which showed little effect for some of the groups. The principal component scores plot indicated five clusters of urine NMR spectra in PC1 and PC2, corresponding to the control group and each of the four high dose treated groups. Good separation with some overlap at the group boundaries was observed in PC1 and PC2 for all four compounds, with some overlap between the PPARα agonists GWα and fenofibrate (light blue and green, respectively, on Figure 1D).

A similar analysis (Figure 1E) was carried out after removal of the 8–48 h samples, as they did not show any separation from controls. At the same time, the groups were resolved further with the use of orthogonal signal correction (Wold *et al*. 1998). The PPARγ agonist (dark blue on Figure 1E) mapped furthest from the controls and the other treated groups. The corresponding loadings plot for this combined data is shown in Figure 2. The loadings in the bottom left quadrant of the plot are present in higher concentrations in the samples that are in the bottom

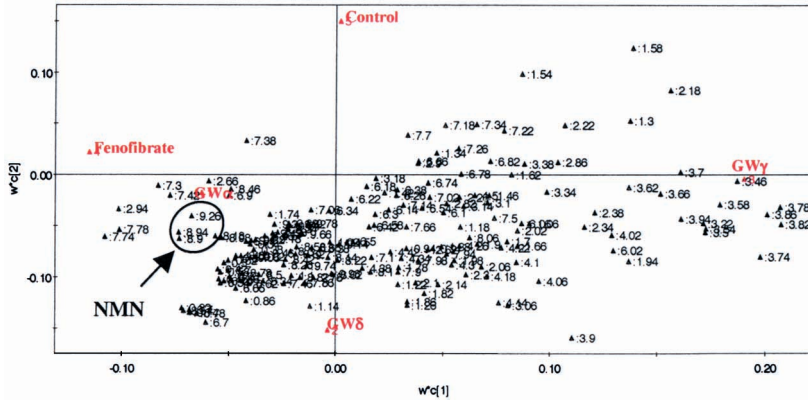

Figure 2. Loadings plot showing the distribution of the ^{1}H NMR regions in relation to the samples shown on the scores plot in Figure 1E. The dose groups are shown in red. Loadings corresponding to NMN are circled.

left quadrant of the scores plot illustrated in Figure 1E than in those in the top right of the scores plot.

In order to construct a table of potential biomarkers of PPAR activity, PLS-DA was then carried out for each compound against its matched control. In the case of each compound, the separation was good (see Figure 1F for fenofibrate), and the first component in each model confirmed that the NMR data contained information about the dose group. This accounted for 45%, 47%, 39% and 47% of the NMR data for GWα, GWδ, GWγ and fenofibrate, respectively.

Among the major spectral regions that discriminate between each dose group when modelled separately against the control group, the spectral regions corresponding to NMN and one of its oxidation products 4PY, were strongly associated with the PPARα agonists GWα and fenofibrate, and to a lesser extent with the PPARδ agonist, but not at all with the PPARγ agonist. There are also unassigned regions, which are possibly related to nicotinic acid metabolites, seen in the spectra of the GWα, GWδ and fenofibrate groups. An extended in-depth statistical analysis of all the changes in the NMR urinary dataset is ongoing.

Detailed analysis of individual urine NMR spectra

Detailed analysis of individual urine spectra confirmed that there were a number of endogenous metabolites with altered levels in urines of animals treated with GWα, GWδ and fenofibrate, whereas their levels remained unaffected in the group treated with GWγ. Structures of two of the most important endogenous metabolites, NMN and 4PY, were confirmed by NMR analysis as follows. NMN was assigned to the ^{1}H resonances at δ 4.47 (s), 9.27 (s), 8.89 (d), 8.19 (t) and 8.95 (d) based on analysis of the 2D ^{1}H-^{1}H TOCSY and 2D ^{1}H-^{13}C HSQC and HMBC NMR spectra of rat urine after treatment with high doses of GWα, and confirmed by comparison with the ^{1}H NMR spectrum of a synthetic standard. 4PY was assigned to the ^{1}H resonances at δ 3.90 (s), 8.54 (d), 6.69 (d) and 7.82 (dd) using similar techniques. Figure 3 shows representative spectra demonstrating the increase in NMN and 4PY following treatment with high dose GWα (Figure 3A) and the absence of changes in the levels of these metabolites following treatment with high dose GWγ (Figure 3B).

Time course study of the urinary excretion of NMN and 4PY metabolites

Concentrations. Concentrations of NMN and 4PY estimated by ^{1}H NMR were compared throughout the 7 days of the study in the urine of both control and treated animals. Initial concentrations of NMN were in the range 15–51 μM when all seven groups were considered over the three 8 h periods prior to dosing (Table 5). On day 6, markedly increased levels of NMN were observed in the groups administered high dose GWα, GWδ and fenofibrate. Throughout the study, NMN concentrations increased in the high dose groups by 17- to 28-fold relative to control (depending on the period of urine collection) with GWα, 16- to 59-fold with fenofibrate, and 6.6- to 19-fold with GWδ. An increase of only 1- to 1.4-fold was observed in the groups treated with high dose GWγ.

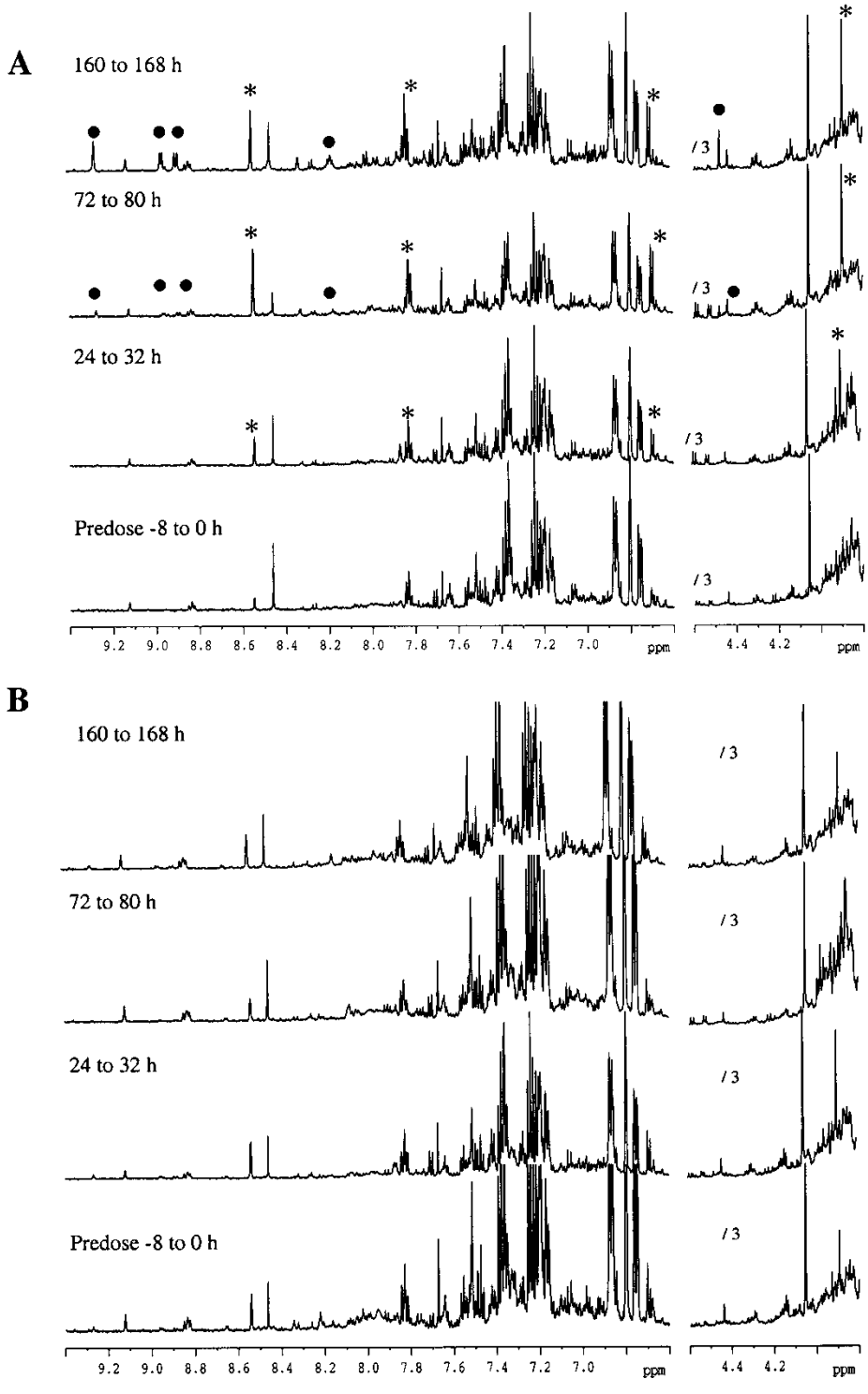

Figure 3. Partial 600 MHz ^{1}H NMR spectra of urine: (A) following high doses of GWα, showing increased levels of NMN (●) and 4PY (*); (B) following high doses of GWγ, showing no changes in NMN or 4PY. /3, signal intensity divided by 3.

Table 5. Fold increases in NMN and 4PY urinary concentrations from day −1 to day 6: ratio of concentrations on day 6 to day −1 for each treated group ($n = 5$), normalized to the concurrent control for each of the three 8 h periods.

		8 a.m. to 4 p.m.		4 p.m. to 12 p.m.		12 p.m. to 8 a.m.	
Treatment	Dose	NMN	4PY	NMN	4PY	NMN	4PY
GWα	Low	2.7	1.4	3.8	1.9	2.5	2.0
	High	17.9	2.6	28.1	3.3	16.5	5.1
GWδ	Low	1.9	1.4	4.0	2.4	2.3	2.2
	High	18.7	2.8	9.6	2.8	6.6	3.4
GWγ	Low	1.2	1.1	2.3	1.7	1.2	1.2
	High	1.4	0.9	1.3	1.2	1.0	1.0
Fenofibrate	Low	4.0	1.4	3.5	2.5	2.2	2.5
	High	58.5	2.5	29.3	2.8	15.9	3.0

Initial concentrations of 4PY were in the range 173–473 μM when all seven groups were considered over the three 8 h periods prior to dosing (Table 5). On day 6, increased levels of 4PY were observed with GWα, GWδ and fenofibrate. Throughout the study, 4PY concentrations in the high dose groups by 2.6- to 5.1-fold relative to control with GWα, 2.5- to 3.0-fold with fenofibrate, and 2.8- to 3.4-fold with GWδ, whereas an increase of only 0.9- to 1.2-fold was observed with GWγ.

Daily excretion. The time course of NMN and 4PY daily excretion is illustrated in Figure 4. Throughout the study, NMN excretion increased (ratio of day 6 to day 1, normalized over the concurrent control ratio) by 17-, 9.5- and 24-fold following high dose GWα, GWδ and fenofibrate, respectively, whereas increases of only 1- to 3-fold were observed in all other groups/doses.

Throughout the study, 4PY excretion also increased (ratio of day 6 to day 1, normalized over the concurrent control ratio) by 3.4-, 3.5- and 3.2-fold following high doses of GWα, GWδ and fenofibrate, respectively, whereas increases of only 1.1- to 2.4-fold were observed in all other groups/doses. Much lower increases were observed with 4PY compared with NMN. A similar observation has been reported by Shibata *et al*. (1996a) after administration of clofibrate to rats: there were increased levels of urinary 4PY and NMN (expressed in nmol day^{-1}), the most striking increase being observed in NMN excretion (increases of approximately 2–3-fold and 30-fold relative to control for 4PY and NMN, respectively).

The time course study of NMN and 4PY urinary excretion confirms the MVDA findings. Significantly increased levels of NMN and 4PY were only observed in animals treated with high doses of GWα, GWδ and fenofibrate, but not with the PPARγ agonist. Where changes in the excretion of NMN and 4PY were observed, levels did not vary simultaneously. There was an initial increase in 4PY excretion beginning on day 1. When levels of 4PY reached approximately 60 μmol kg^{-1} per 24 h, levels of NMN started to increase. Levels of 4PY then remained constant, which suggests that the 4PY-forming oxidase may be saturated. It has also been reported that the hepatic activity of the 2PY- and 4PY-forming oxidases (*N*-methylnicotinamide oxidases, EC 1.2.3.1), which convert NMN to 2PY and 4PY,

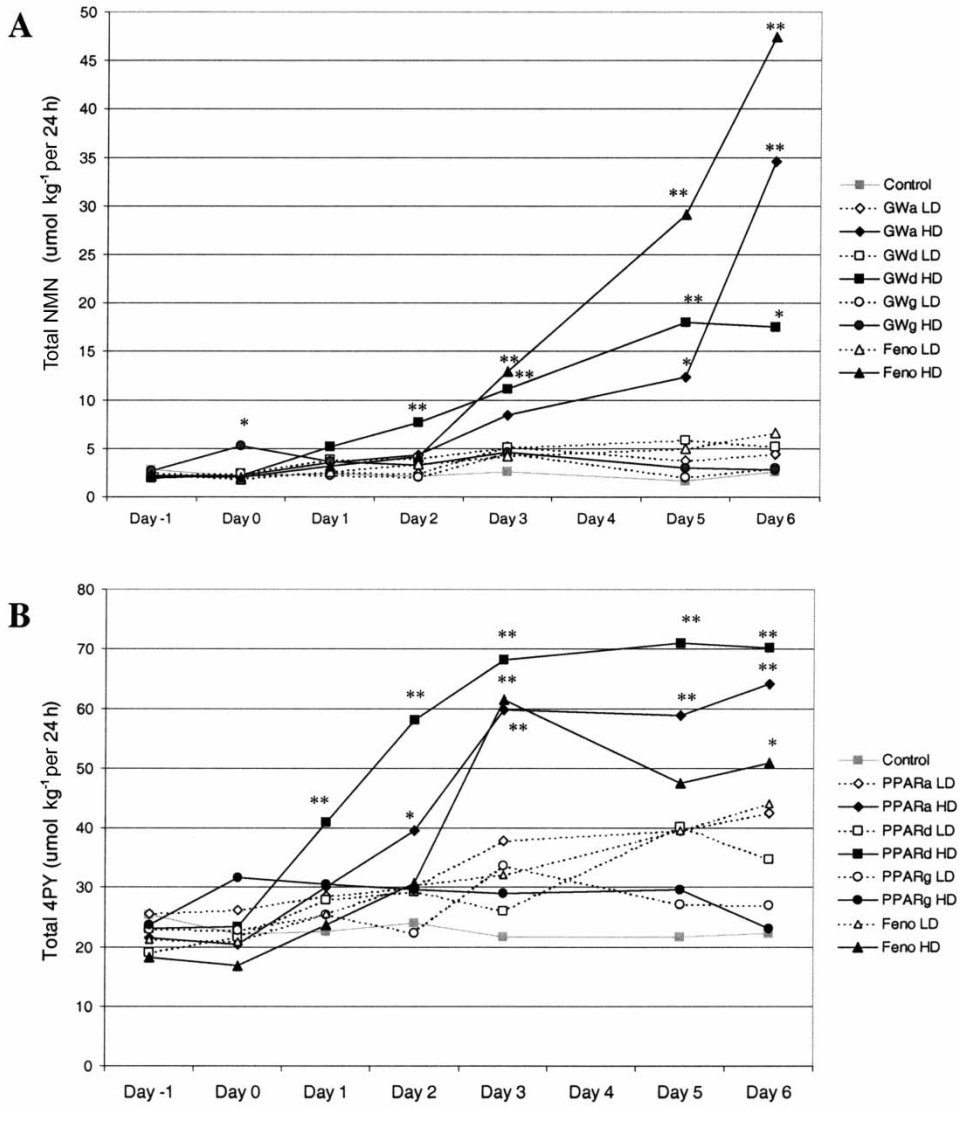

Figure 4. Time course of NMN (A) and 4PY (B) mean daily urinary excretion for all groups ($n = 5$ per group) from day -1 until day 6. There are no data for day 4 due to a missing urine volume for one of the collection periods. GWa, GWα; GWd, GWδ; GWg, GWγ; Feno, fenofibrate; LD, low dose; HD, high dose. $^{*}p < 0.05$; $^{**}p < 0.01$.

respectively, decreased following an intraperitoneal dose of nicotinamide or NMN to rats, leading to a decreased ratio of 2PY plus 4PY to NMN excretion (Shibata and Matsuo, 1989a,b).

Urinary excretion of nicotinamide and its metabolites as reported in the literature. Most data published in the literature on NMN urinary levels are expressed as nmol g^{-1} diet, since the food intake differs from one animal to the other (Shibata *et al*. 1996b, Fukuwatari *et al*. 2002), and therefore these data cannot be compared with

our estimations. The urinary concentrations of NMN and 4PY in the current study are consistent with those measured by HPLC and reported as 9.74 ± 2.60 and 52.60 ± 9.74 μmol kg^{-1} per 24 h, respectively, in male control Wistar rats (Shibata 1989).

In control Wistar rats, 4PY has been shown to be the most abundant urinary metabolite of nicotinamide (Shibata *et al*. 1990), the proportions being 82% 4PY, 7% NMN, 7% 2PY, 4% nicotinamide and up to 1% nicotinamide *N*-oxide, with no niacin or nicotinuric acid. The metabolites 6-hydroxynicotinamide, 6-hydroxynicotinic acid and *N*-methylnicotinic acid (trigonelline) have also been identified in rat urine (Lee *et al*. 1969, Yuyama and Suzuki 1985).

Diurnal variation. Diurnal variations in the excretion of NMN and 4PY were also investigated to determine whether urine should be collected over a specific period of the day. In the control group, the combined mean excretion of NMN and 4PY, as well as the urine volumes excreted, over each of the three 8 h periods showed diurnal variation, whilst the mean concentration remained constant (Table 6). Contrary to what one would expect, the urinary concentration of NMN and 4PY did not increase during periods when a lower volume of urine was excreted (i.e. the 8 a.m. to 4 p.m. periods). The lower rate of excretion between 8 a.m. and 4 p.m. coincides with the time of least feeding and physical activity. As there is no time period when NMN and 4PY urinary concentrations are higher, no specific period of the day appears to be more suitable for urine collection.

NMR analysis of plasma

Following visual inspection of ^{1}H NMR spectra of plasma samples from all animals, no drug-related metabolites were seen. MVDA did not identify any changes except: (i) decreased lipid levels for all treatments (with the exception of low dose GWδ) as expected from clinical chemistry findings; and (ii) decreased lactate levels for all treatments (lactate has been shown to be one of the most variable metabolites in rat plasma; Deprez *et al*. 2003).

The two nicotinamide metabolites NMN and 4PY identified in the urine of some of the treated animals were not detected in the corresponding plasma samples (Figure 5A). It was confirmed that no NMN was lost through protein binding in plasma samples, which is consistent with the findings of Ross *et al.* (1975). It appears that the circulating levels of nicotinamide metabolites in plasma were below the limit of detection provided by ^{1}H NMR analysis, as none of the nicotinamide metabolites were visible in the rat plasma on ^{1}H NMR. Although ^{1}H NMR is able to detect most small proton-containing metabolites without prior selection, it is not a very sensitive method for identifying metabolites, nor is it easy to quantify metabolites once they have been identified (the limit of detection at 700 MHz was estimated to be 2 μM in a 0.5 ml sample volume). More sensitive methods to quantify levels of nicotinamide metabolites in plasma are required.

Determination of NMN levels in plasma using HPLC spectrofluorimetry

Although 4PY is an endpoint of nicotinamide metabolism and therefore a good candidate for a urinary biomarker of peroxisome proliferation in the rat, the relative

Table 6. Diurnal variation in the combined (NMN+4PY) urinary excretion over the three 8 h periods in control animals ($n = 5$) on day 1 and day 6 (mean data and two-way ANOVA comparing the three time periods).

	Day 1				Day 6			
	8 a.m. to 4 p.m.	4 p.m. to 12 p.m.	12 p.m. to 8 a.m.	ANOVA	8 a.m. to 4 p.m.	4 p.m. to 12 p.m.	12 p.m. to 8 a.m.	ANOVA
Amount excreted (μmol kg^{-1} per 8 h per animal)	1.78	14.9	11.5	$p < 0.05$	1.46	10.8	12.5	$p < 0.01$
Concentration (μM)	288	425	308		319	341	346	
Urine volume excreted (ml per animal)	2.0	10.6	10.4	$p < 0.01$	1.4	9.8	11.6	$p < 0.01$

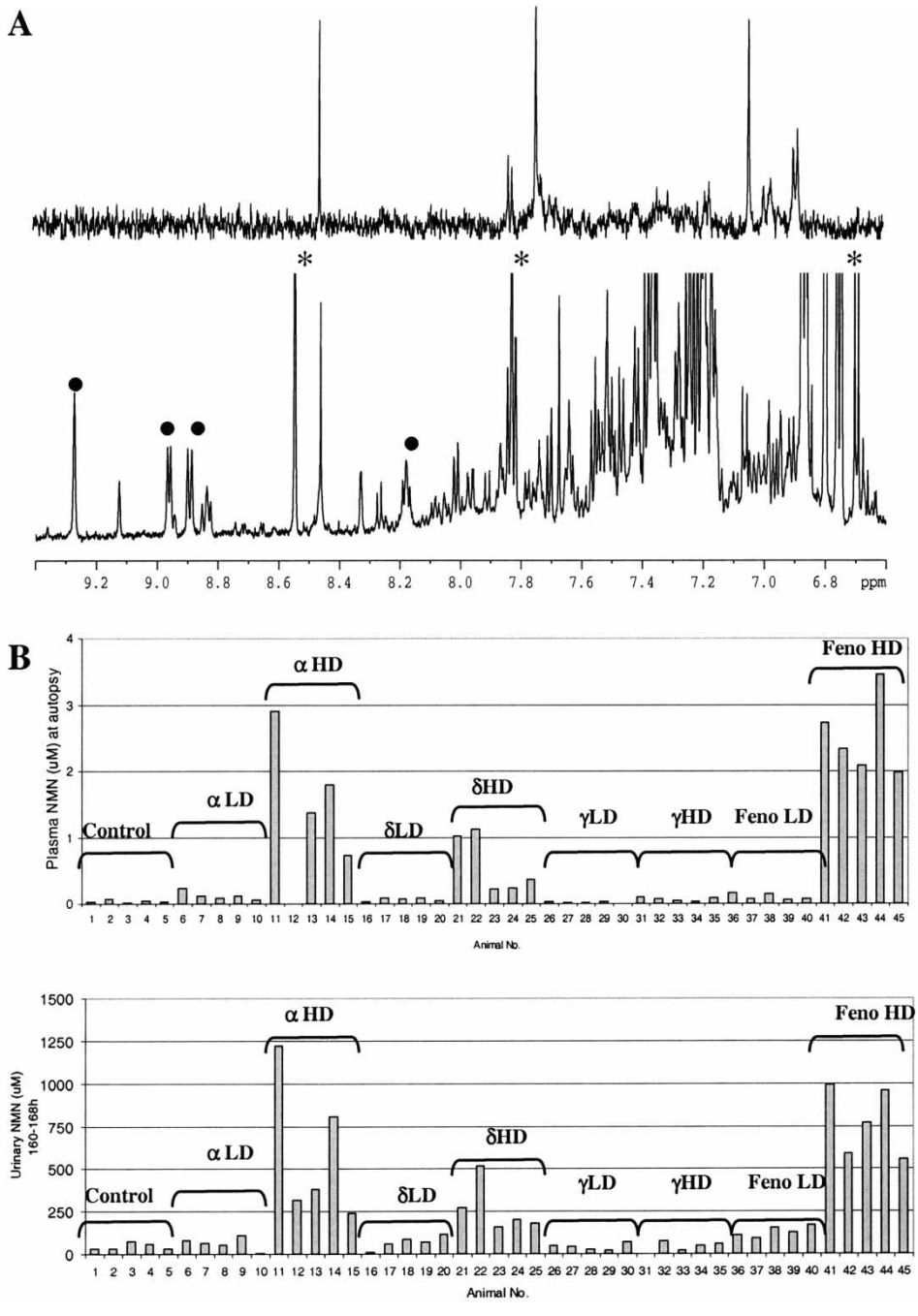

Figure 5. (A) Partial 600 MHz ^{1}H NMR spectra of biofluids collected on day 7 after high dose GWα. Top panel: plasma – NMN and 4PY not detected. Bottom panel: urine – increased levels of NMN (●) and 4PY (*) compared with predose values. (B) NMN concentrations in biofluids from individual animals at the end of the study. Top panel: plasma analysed by HPLC spectrofluorimetry (results are the mean of duplicates; animal no. 12, missing sample). Bottom panel: urine collected 8 h before autopsy (day 7, 12 p.m. to 8 a.m.) and analysed by ^{1}H NMR. LD, low dose; HD, high dose; α, GWα; δ, GWδ; γ, GWγ; Feno, fenofibrate.

fold increase in NMN excretion following treatment makes it potentially a better biomarker than 4PY. Plasma levels of NMN are expected to increase when there is increased hepatic production of nicotinamide metabolites and no increase in the renal clearance of NMN. As there was no evidence of kidney lesions by histopathology or clinical chemistry, it was unlikely that the increased urinary NMN was due to altered renal handling.

Plasma samples prepared at autopsy were analysed using an HPLC spectrofluorimetric method (adapted from Musfeld *et al.* 2001). The results are illustrated in Figure 5B (top panel) and Table 7. The mean plasma concentration of NMN at autopsy in the control group was approximately 1000-fold lower than the corresponding NMN concentration in control urine. No other data on NMN levels in control rat plasma appear to have been reported.

Although there was variability in the data between animals, significant increases were observed in animals treated with high dose GWα and fenofibrate compared with the control group (Table 7). Interestingly, the changes in NMN levels in plasma at autopsy correlated well ($r^2 = 0.93$) with the NMN urinary levels in the 8 h collection period prior to autopsy (Figure 5B). This supports the hypothesis that increased NMN urinary levels are the consequence of an increased hepatic production of NMN rather than altered renal handling.

Possible mechanism involved: the tryptophan-NAD$^+$ pathway

The two metabolites identified as potential markers of peroxisome proliferation, NMN and 4PY, are end products of nicotinamide metabolism in the liver (Figure 6). Nicotinamide is the amide derivative of nicotinic acid (niacin or vitamin B3), a vitamin involved in the tryptophan-NAD$^+$ pathway, which supplies pyridine nucleotides to the liver. Nicotinamide is partly catabolized to NMN via nicotinamide *N*-methyltransferase (EC 2.1.1.1), and is subsequently catabolized to 2PY and 4PY via aldehyde oxidase (EC 1.2.3.1) (Wolf 1974).

Excess tryptophan in the diet is normally metabolized via the kynurenine pathway to 2-amino-3-carboxymuconate semialdehyde (ACMS), an unstable intermediate, which is further metabolized to CO_2, NH_3 and energy through the oxidative glutarate pathway, the key enzyme being ACMSD (EC 4.1.1.45, formerly

Table 7. Mean ($n = 5$) plasma levels of NMN measured by HPLC spectrofluorimetry in all groups at necropsy and comparison of treated groups with the control group.

		Plasma NMN (nM)			
Treatment	Dose	Mean	SEM	Fold increase over control	Dunnett's test
Control		41.3	9.6		
GWα	Low	122	30	2.9	
	High	1704	458	41.3	$p < 0.01$
GWδ	Low	65.3	11.3	1.6	
	High	592	200	14.3	
GWγ	Low	13.3	6.4	0.3	
	High	70.8	13.0	1.7	
Fenofibrate	Low	102	22	2.5	
	High	2518	267	61.0	$p < 0.01$

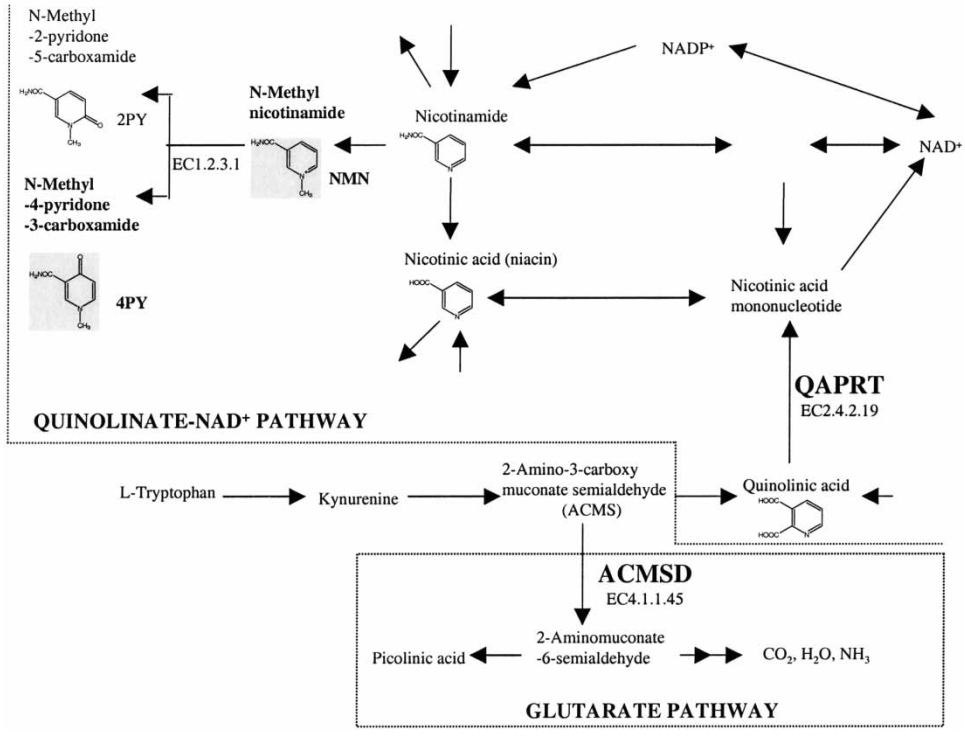

Figure 6. The tryptophan-NAD$^+$ pathway, including the glutarate pathway and the quinolinate-NAD$^+$ pathway and showing the endproducts NMN and 4PY.

termed picolinic carboxylase). This enzyme catalyses the first step of the formation of acetyl CoA from ACMS. Small amounts of ACMS spontaneously cyclize to form quinolinic acid and, via the enzyme QAPRT (EC 2.4.2.19), nicotinic acid, NAD$^+$ or other catabolites (Brown 1994). QAPRT is a key, rate-limiting enzyme in the formation of NAD$^+$ from ACMS. QAPRT activity has been reported to be higher in the liver (Ikeda *et al*. 1965), whereas ACMSD activity has been shown to be higher in the kidney (Ikeda *et al*. 1965, Fukuwatari *et al*. 2001). NMN and its metabolites have been reported to be increased in response to the increased flux of tryptophan to NAD$^+$ when the metabolism of tryptophan via the glutarate pathway was blocked by reduced hepatic activity of ACMSD (Shibata *et al*. 1996a, Shin *et al*. 1998a). Excess nicotinamide was excreted mainly as NMN and 4PY in rat urine (Shibata *et al*. 1990). Thus the gene expression of QAPRT and ACMSD was examined in liver tissue.

Evidence of a link with the tryptophan-NAD$^+$ pathway: QAPRT and ACMSD gene expression in liver tissue

Genomic investigations were carried out on liver tissues collected from three of the five animals treated with high doses of GWδ, GWγ and fenofibrate using the Clontech rat ToxII array platform. However, no liver gene changes in relation to the tryptophan-NAD$^+$ pathway were detected (data not shown). Therefore, subsequent analysis was targeted to look at ACMSD and QAPRT gene expression using

quantitative real-time RT-PCR (TaqMan®) in liver tissues, as the tryptophan-NAD^+ pathway occurs in the liver in the rat (Fukuwatari *et al*. 2001).

While most authors have studied changes in ACMSD and/or QAPRT liver activity in rats after various treatments, few authors have measured the liver mRNA of these enzymes. Egashira *et al.* (1998) reported decreased ACMSD activity reflected in a decrease in ACMSD protein levels in rats fed linoleic acid. In rats given a high protein diet and those with streptozotocin-induced diabetes, an increase in hepatic ACMSD mRNA expression was followed by an increase in ACMSD activity (Tanabe *et al*. 2002).

The only significant changes in QAPRT mRNA expression in this study were a slight increase following high doses of fenofibrate and a slight decrease following a

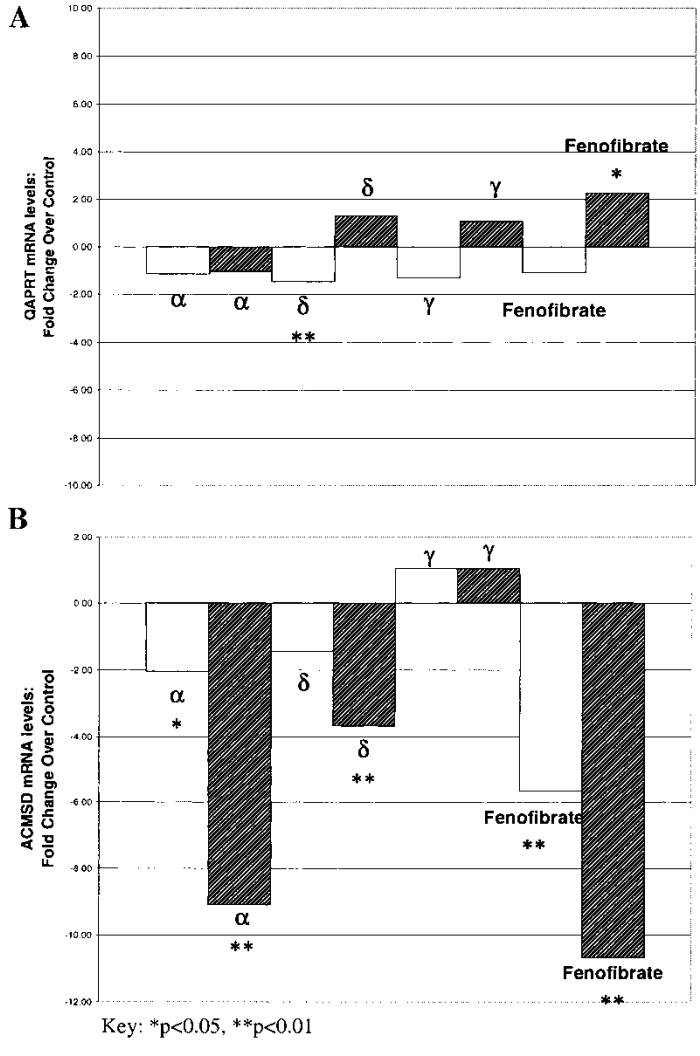

Figure 7. mRNA levels of QAPRT (A)and ACMSD (B) in liver tissue at autopsy, expressed as mean fold change over control ($n = 5$, data normalized to 18S ribosomal RNA). Open columns, low dose; shaded columns, high dose; α, GWα; δ, GWδ; γ, GWγ.

low dose of GWδ (Figure 7A). The biological significance of the latter observation is currently unknown, as the mean fold change over control values was less than 2. However, a marked significant decrease in ACMSD mRNA expression was observed in livers from animals treated with high doses of GWα and fenofibrate (9.1- and 10.7-fold normalized change over control, respectively) (Figure 7B). Some downregulation was also observed following treatment with low doses of fenofibrate and GWα, and high doses of GWδ. No downregulation of ACMSD was seen in the group treated with GWγ. This targeted approach using TaqMan® to assess specific genes proved very useful in supporting the contention of an alteration in the tryptophan-NAD^+ pathway after treatment with the PPARα agonists.

Correlation of cumulative NMN urinary excretion with liver weight and peroxisome frequency

In order to determine whether urinary NMN was a possible surrogate marker for peroxisome proliferation in the rat, its cumulative excretion over the 7 days of the study was compared to two endpoints of peroxisome proliferation: relative liver weight and peroxisome count at autopsy. Correlations were also made with lipid parameters to determine whether changes in NMN simply reflect the pharmacology (lipid changes) of the compounds administered. Liver weights were expressed relative to body weights, thereby minimizing the effect of inter-animal variation. In addition, the NMN values were log-transformed (log), and peroxisome counts were square-root transformed (sqrt) (which is standard practice for all data involving counts), so that the variables were distributed more normally. There was a high level of correlation between log NMN and sqrt peroxisome count (Table 8 and Figure 8), and also between log NMN and the relative liver weight (Table 8). The correlations between log NMN and cholesterol, TRG, HDL and LDL were less than that between the peroxisome counts.

Except for GWγ, there was strong statistical evidence of an increase for all three endpoints (log NMN, sqrt peroxisome count and relative liver weight) against control values for all the high dose groups (Dunnett's test) (Table 9).

These results suggest that the three endpoints agreed with each other well, and that NMN was a suitable endpoint of peroxisome proliferation. However, none of the four compounds showed any strong evidence of an increase at low doses, for any of the three endpoints; there was some evidence of this, although it was only marginal at the 5% level of significance with low dose fenofibrate with log NMN

Table 8. Correlation between NMN urinary excretion (expressed as cumulative excretion in μmol kg^{-1} per 7 days and log-transformed) and other endpoints measured at autopsy ($n = 5$).

Endpoints for comparison with log NMN	Correlation coefficient r
sqrt peroxisome count	0.87[a]
Relative liver weight	0.79
Plasma cholesterol	−0.61
Plasma TRG	−0.37
Plasma HDL	−0.63
Plasma LDL	−0.30

[a] $n = 2$.

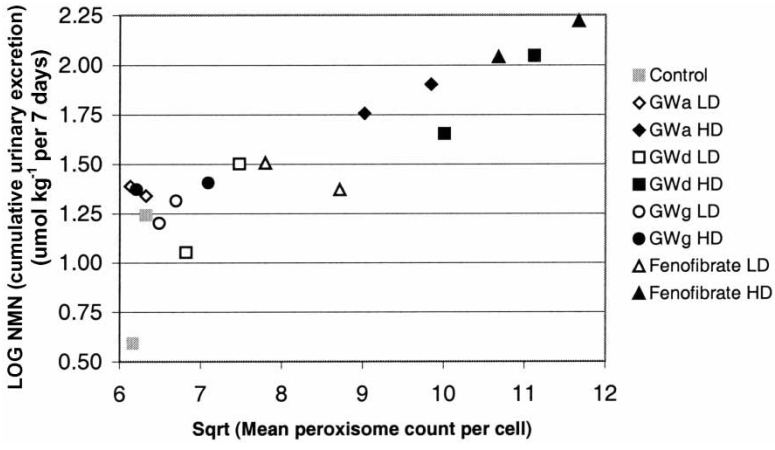

Figure 8. Correlation between NMN urinary excretion and peroxisome count (data expressed as the mean per cell and square-root transformed). GWa, GWα; GWd, GWδ; GWg, GWγ; LD, low dose; HD, high dose.

Table 9. Dunnett's test p values for three endpoints: relative liver weight ($n = 5$), NMN urinary excretion ($n = 5$, data expressed as cumulative urinary excretion in μmol kg^{-1} per 7 days and log-transformed) and mean peroxisome count ($n = 2$, data expressed as mean for periportal and centrilobular regions per cell and square-root transformed).

Treatment	Dose	Relative liver weight	log NMN	sqrt peroxisome count
GWα	Low	0.3807	0.1483	0.8957
	High	< 0.0001**	< 0.0001**	0.0006**
GWδ	Low	0.7942	0.0254	0.2390
	High	< 0.001**	< 0.001**	< 0.0001**
GWγ	Low	0.9995	0.5030	0.6685
	High	1.0000	0.0663	0.6208
Fenofibrate	Low	0.7861	0.0312*	0.0115*
	High	< 0.001**	< 0.001**	< 0.0001**

*$p < 0.05$; **$p < 0.01$.

and sqrt peroxisome count, and with low dose GWδ with the log NMN endpoint only.

Conclusions

The observations in this study are consistent with other reports in the literature in which the altered flux in the tryptophan-NAD^+ pathway has been shown to be controlled by the altered activity of ACMSD and QAPRT.

Studies where upregulation in the tryptophan-NAD^+ pathway has been investigated following treatment with PPAR ligands

A number of studies have been reported by Shibata *et al*. and Shin *et al*. that have focussed on the alteration of the tryptophan-NAD^+ pathway by compounds including PPAR ligands (clofibrate being used in most studies), in rats (Shibata *et al*. 1996a; Shin *et al.* 1999a) or rat hepatocytes (Shin *et al*. 1996, 1998c, 1999b), at

doses reported to cause peroxisome proliferation. They identified reduced hepatic activity of ACMSD and increased hepatic activity of QAPRT as the controlling mechanism for these changes. They also examined the ratios of NAD^+ to reduced NAD (NADH) and of NAD phosphate ($NADP^+$) to reduced NAD phosphate (NADPH). An increase in NAD^+ synthesis in the liver was reported following increased activity of QAPRT; a concomitant decrease in the activity of ACMSD was also observed. In studies with clofibrate, it was proposed that this peroxisome proliferator might affect transcription of genes encoding key enzymes in the tryptophan-NAD^+ pathway in relation to the PPARs expressed by the administration of clofibrate. Clofibrate may decrease the biosynthesis of the ACMSD protein and/or mRNA (Shibata *et al*. 1996a). The conversion ratio of tryptophan to niacin was shown to increase, for instance with increasing dietary concentrations of di-(2-ethylhexyl)phthalate (DEHP), a peroxisome proliferator in the rat (Fukuwatari *et al*. 2002). The authors suggested that the inhibition of ACMSD activity or gene expression by DEHP or its metabolites was responsible for this effect.

Using radioisotopes, Shin *et al.* (1996) demonstrated that the increase in NAD^+ in hepatocytes treated with clofibrate was due to an acceleration of NAD^+ synthesis, not a retardation of degradation. The decrease in the NAD^+:NADH ratio (a greater increase in NADH than in NAD^+) and the increase in hydrogen peroxide produced indicated that fatty acid oxidation was stimulated in the liver of rats fed clofibrate or DEHP (Shin *et al*. 1998a, 1999b). However, when inhibitors of hepatic peroxisomal fatty acid oxidation (phenothiazines) were co-administered to rats fed a clofibrate diet, the necessary cofactor NAD^+ was still increased, suggesting the increase in NAD^+ was not related directly to the metabolism of fatty acids in peroxisomes (Shin *et al.* 1998b), although it may be stimulated by increased levels of fatty acids. Clofibrate was shown not to have any inhibitory activity on ACMSD enzymatic activity (Shin *et al*. 1998a).

The mechanism linking tryptophan-NAD^+ enzyme induction/regulation with peroxisome proliferation is not known. In the absence of any firm evidence, the mode of action of PPAR ligands points to a possible co-activation and/or co-repression of genes coding for the enzymes involved in the tryptophan-NAD^+ pathway. This influence on other genes could involve not only the direct activation or repression of the actual genes that code for the enzymes in the tryptophan-NAD^+ pathway, but also indirect activation or repression of the transcription of activators, repressors, transcription factors or binding proteins involved in the signalling cascade. Shin *et al.* (1999a) refers to such a possible indirect influence on ACMSD.

Other studies not including PPARs ligands where upregulation in the tryptophan-NAD^+ pathway has been investigated

Increases in biofluid and tissue nicotinamide and/or metabolites have been reported in relation to cirrhosis in humans (Cuomo *et al*. 1995, Pumpo *et al*. 2001). However, the mechanism leading to this increase seems to be different from that involved with PPAR ligands. The first step in the perturbation of the NAD^+ pathway was possibly a decrease in the ATP available for NAD^+ synthesis (Cuomo *et al*. 1995). Nicotinamide could no longer be transformed into NAD^+, it

accumulated in cells, and was detoxified through methylation to NMN. When liver injury was induced in rats with galactosamine, there was a decrease in ACMSD liver activity, which resulted in an increase in urinary nicotinamide (Egashira *et al*. 1997). However, none of the studies involving changes in the tryptophan-NAD^+ pathway appear to result in the same levels of NMN seen with PPARα activity (Table 10).

Polyunsaturated fatty acids (PUFA) fed to rats decreased ACMSD activity and protein levels in liver (Egashira *et al*. 1992, 1994, 1998). One possible explanation was the inhibition of ACMSD by the peroxide produced through oxidation of PUFA. Following the study of NMN excretion patterns in patients with leukaemia, NMN has been described as a tentative prognostic indicator of recovery (Tamulevicius and Streffer 1984). In none of these studies was a marked rise in urinary NMN seen.

Final conclusion

The studies mentioned above support the hypothesis that ACMSD provides a control mechanism for the formation of NAD^+ from tryptophan, as already reported by Wolf (1974). The branch point of ACMSD was described by Brown (1994) as 'a locus of regulation of quinolinic acid and hence NAD synthesis'. We suggest that the upregulation of this pathway is in response to an increase in the demand for NAD^+ for the β-oxidation of long-chain fatty acids. Any inefficiency in the oxidative process is likely to result in excess NAD^+, which will be excreted as NMN and 4PY in the rat. However, more work needs to be done to understand

Table 10. Studies where increased levels of NMN have been estimated in urine or plasma from rats or humans following various treatments/diseases.

	Fold-increase relative to control		
Condition	Urinary NMN	Plasma NMN	Reference
In the rat			
PPAR ligands dosed to rats			
GWα, high dose	17–28[a]	41	This study
GWδ, high dose	6.6–19[a]	14	This study
Fenofibrate, high dose	16–59[a]	61	This study
Clofibrate fed to rats	~30		Shibata *et al*. 1996a
Studies in rats that did not involve PPAR ligands	2–8		
Stressed rat liver		2[b]	Cuomo *et al*. 1995
Liver injury in rats (galactosamine)	2		Egashira *et al*. 1997
Nitrate/nitrite exposure in rats	2		Jansen *et al*. 1995
In humans			
Nitrate/nitrite exposure	0–6		Jansen *et al*. 1995
Indicator of recovery from leukaemia	2–5		Tamulevicius and Streffer 1984
Cirrhosis	3	2	Pumpo *et al*. 2001

Data correspond to increases in NMN concentrations, except for data from Egashira *et al*. (1997) (increase in NMN excretion).

[a]Depending on the period of urine collection.

[b]*In vitro* perfusion.

how PPAR ligands modulate the tryptophan-NAD^+ pathway and hence the hepatic production of nicotinamide metabolites.

This work has highlighted the power of using metabonomics in the identification of potential biomarkers of subtle cellular changes. The evidence is consistent with NMN and 4PY being potential non-invasive biomarkers of peroxisome proliferation that can be measured in urine and plasma. Investigations are being carried out to see whether these biomarkers or other metabolites in the same pathway are able to predict peroxisome proliferation in different species, including humans.

Acknowledgements

The authors acknowledge GlaxoSmithKline Pharmaceuticals (UK) for the funding of this work. Stephanie Ringeissen also received the financial support of the EU as part of the Marie Curie Industry Host Fellowship Programme.

References

Ashby, J., Brady, A., Elcombe, C. R., Elliott, B. M., Ishmael, J., Odum, J., Tugwood, J. D., Kettle, S. and Purchase, I. F. H. 1994, Mechanistically-based human hazard assessment of peroxisome proliferator-induced hepatocarcinogenesis. *Human and Experimental Toxicology*, **13** (Supplement 2), S1–S117.

Beier, K. 1992, Light microscopic morphometric analysis of peroxisomes by automatic image analysis: advantages of immunostaining over the alkaline DAB method. *Journal of Histochemistry and Cytochemistry*, **40**, 115–121.

Bentley, P., Calder, I., Elcombe, C., Grasso, P., Stringer, D. and Wiegand, H. J. 1993, Hepatic peroxisome proliferation in rodents and its significance for humans. *Food and Chemical Toxicology*, **31**, 857–907.

Bernofsky, C. 1979, New synthesis of the 4- and 6-pyridones of 1-methylnicotinamide and 1-methylnicotinic acid (trigonelline). *Analytical Biochemistry*, **96**, 189–200.

Brown, R. R. 1994, Tryptophan metabolism: a review. In *L-Tryptophan: Current Prospects in Medicine and Drug Safety*, edited by W. Kochen and H. Steinhart (Berlin: Walter de Gruyter & Co), pp. 17–30.

Bybee, A., Styles, J. A., Beck, S. L. and Blackburn, D. 1990, Mitosis and histopathology in rat liver during methylclofenapate induced hyperplasia. *Cancer Letters*, **52**, 95–100.

Cuomo, R., Pumpo, R., Sarnelli, G., Capuano, G. and Budillon, G. 1995, Nicotinamide methylation and hepatic energy reserve: a study by liver perfusion in vitro. *Journal of Hepatology*, **23**, 465–470.

DeLuca, J. G., Doebber, T. W., Kelly, L. J., Kemp, R. K., Molon-Noblot, S., Sahoo, S. P., Ventre, J., Wu, M. S., Peters, J. M., Gonzalez, F. J. and Moller, D. E. 2000, Evidence for peroxisome proliferator-activated receptor (PPAR)alpha-independent peroxisome proliferation: effects of PPARgamma/delta-specific agonists in PPARalpha-null mice. *Molecular Pharmacology*, **58**, 470–476.

Deprez, S., Sweatman, B. C., Connor, S. C., Haselden, J. N. and Waterfield, C. J. 2003, Optimisation of collection, storage and preparation of rat plasma for 1H NMR spectroscopic analysis in toxicology studies to determine inherent variation in biochemical profiles. *Journal of Pharmaceutical and Biomedical Analysis*, **30**, 1297–1310.

Dunnett, C. W. 1955, A multiple comparisons procedure for comparing several treatments with a control. *Journal of the American Statistical Association*, **50**, 1096–1121.

Egashira, Y., Yamamiya, Y. and Sanada, H. 1992, Effects of various dietary fatty acids on α-amino-β-carboxymuconate-ε-semialdehyde decarboxylase activity in rat liver. *Bioscience, Biotechnology, and Biochemistry*, **56**, 2015–2019.

Egashira, Y., Ogawara, R., Ohta, T. and Sanada, H. 1994, Suppression of hepatic α-amino-β-carboxymuconate-ε-semialdehyde decarboxylase (ACMSD) activity by linoleic acid in relation to its induction by glucocorticoids and dietary protein. *Bioscience, Biotechnology, and Biochemistry*, **58**, 339–343.

Egashira, Y., Komine, T., Ohta, T., Shibata, K. and Sanada, H. 1997, Change of tryptophan-niacin metabolism in D-galactosamine-induced liver injury in rat. *Journal of Nutritional Science and Vitaminology*, **43**, 233–239.

EGASHIRA, Y., TANABE, A., OHTA, T. and SANADA, H. 1998, Dietary linoleic acid alters alpha-amino-beta-carboxymuconate-epsilon-semialdehyde decarboxylase (ACMSD), a key enzyme of niacin synthesis from tryptophan, in the process of protein expression in rat liver. *Journal of Nutritional Sciences and Vitaminology*, **44**, 129–136.

ELCOMBE, C. R., BELL, D. R., ELIAS, E., HASMALL, S. C. and PLANT, J. P. 1997, Peroxisome proliferators: species differences in response of primary hepatocyte cultures. *Annals of the New York Academy of Sciences*, **804**, 628–635.

FUKUWATARI, T., MORIKAWA, Y., HAYAKAWA, F., SUGIMOTO, E. and SHIBATA, K. 2001, Influence of adenine-induced renal failure on tryptophan-niacin metabolism in rats. *Bioscience, Biotechnology, and Biochemistry*, **65**, 2154–2161.

FUKUWATARI, T., SUZUKI, Y., SUGIMOTO, E. and SHIBATA, K. 2002, Elucidation of the toxic mechanism of the plasticizers, phthalic acid esters, putative endocrine disrupters: effects of dietary di(2-ethylhexyl)phthalate on the metabolism of tryptophan to niacin in rats. *Bioscience, Biotechnology, and Biochemistry*, **66**, 705–710.

HANEFELD, M., KEMMER, C. and KADNER, E. 1983, Relationship between morphological changes and lipid-lowering action of *p*-chlorphenoxyisobutyric acid (CPIB) on hepatic mitochondria and peroxisomes in man. *Atherosclerosis*, **46**, 239–246.

HENKE, B. R., BLANCHARD, S. G., BRACKEEN, M. F., BROWN, K. K., COBB, J. E., COLLINS, J. L., HARRINGTON, W. W. JR, HASHIM, M. A., HULL-RYDE, E. A., KALDOR, I., KLIEWER, S. A., LAKE, D. H., LEESNITZER, L. M., LEHMANN, J. M., LENHARD, J. M., ORBAND-MILLER, L. A., MILLER, J. F., MOOK, R. A. JR, NOBLE, S. A., OLIVER, W. JR, PARKS, D. J., PLUNKET, K. D., SZEWCZYK, J. R. and WILLSON, T. M. 1998, *N*-(2-Benzoylphenyl)-L-tyrosine PPARgamma agonists. 1. Discovery of a novel series of potent antihyperglycemic and antihyperlipidemic agents. *Journal of Medicinal Chemistry*, **41**, 5020–5036.

HOLLINSHEAD, M. and MEIJER, J. 1988, Immunocytochemical analysis of soluble epoxide hydrolase and catalase in mouse and rat hepatocytes demonstrates a peroxisomal localization before and after clofibrate treatment. *European Journal of Cell Biology*, **46**, 394–402.

IARC. 1995, *Peroxisome Proliferation and its Role in Carcinogenesis*. IARC Technical Report No 24 (Lyon: International Agency for Research on Cancer).

IKEDA, M., TSUJI, H., NAKAMUR, S., ICHIYAMA, A., NISHIZUKA, Y. and HAYAISHI, O. 1965, Studies on the biosynthesis of nicotinamide adenine dinucleotide (II). *Journal of Biological Chemistry*, **240**, 1395–1401.

JANSEN, E. H. J. M., VAN DEN BERG, R. H., BOINK, A. B. T. J., HEGGER, C. and MEULENBELT, J. 1995, A new physiological biomarker for nitrate exposure in humans. *Toxicology Letters*, **77**, 265–269.

LAKE, B. G. 1995a, Mechanisms of hepatocarcinogenicity of peroxisome-proliferating drugs and chemicals. *Annual Review of Pharmacology and Toxicology*, **35**, 483–507.

LAKE, B. G. 1995b, Peroxisome proliferation: current mechanisms relating to non-genotoxic carcinogenesis. *Toxicology Letters*, **82–83**, 673–681.

LALWANI, N. D., REDDY, M. K., GHOSH, S., BARNARD, S. D., MOLELLO, J. A. and REDDY, J. K. 1985, Induction of fatty acid β-oxidation and peroxisome proliferation in the liver of Rhesus monkeys by DL-040, a new hypolipidemic agent. *Biochemical Pharmacology*, **34**, 3473–3482.

LEE, Y. C., GHOLSON, R. K. and RAICA, N. 1969, Isolation and identification of two new nicotinamide metabolites. *Journal of Biological Chemistry*, **244**, 3277–3282.

MOODY, D. E., REDDY, J. K., LAKE, B. G., POPP, J. A. and REESE, D. H. 1991, Peroxisome proliferation and non-genotoxic carcinogenesis: commentary on a symposium. *Fundamental and Applied Toxicology*, **16**, 233–248.

MUSFELD, C., BIOLLAZ, J., BELAZ, N., KESSELRIG, U. W. and DECOSTERD, L. A. 2001, Validation of an HPLC method for the determination of urinary and plasma levels of *N*-methylnicotinamide, an endogenous marker of renal cationic transport and plasma flow. *Journal of Pharmaceutical and Biomedical Analysis*, **24**, 391–404.

NICHOLLS, A. W., NICHOLSON, J. K., HASELDEN, J. N. and WATERFIELD, C. J. 2000, A metabonomic approach to the investigation of drug induced phospholipidosis: an NMR spectroscopy and pattern recognition study. *Biomarkers*, **5**, 410–423.

NICHOLSON, J. K., HIGHAM, D. P., TIMBRELL, J. A. and SADLER, P. J. 1989, Quantitative high-resolution ^{1}H NMR urinalysis studies on the biochemical effects of cadmium in the rat. *Molecular Pharmacology*, **36**, 398–404.

NICHOLSON, J. K., LINDON, J. C. and HOLMES, E. 1999, 'Metabonomics': understanding the metabolic responses of living systems to pathophysiological stimuli via multivariate statistical analysis of biological NMR spectroscopic data. *Xenobiotica*, **29**, 1181–1189.

OIKAWA, I. and NOVIKOFF, P. M. 1995, Catalase-negative peroxisomes: transient appearance in rat hepatocytes during liver regeneration after partial hepatectomy. *American Journal of Pathology*, **146**, 673–687.

Pauley, C. J., Ledwith, B. J. and Kaplanski, C. 2002, Peroxisome proliferators activate growth regulatory pathways largely via peroxisome proliferator-activated receptor α-independent mechanisms. *Cellular Signalling*, **14**, 351–358.

Pumpo, R., Sarnelli, G., Spinella, A., Budillon, G. and Cuomo, R. 2001, The metabolism of nicotinamide in human liver cirrhosis: a study on *N*-methylnicotinamide and 2-pyridone-5-carboxamide production. *American Journal of Gastroenterology*, **96**, 1183–1187.

Qualls, C. W., Hoivik, D. J., Santostefano, M. J., Brown, H. R., Anderson, S. P., Ott, R. J., Mirabile, R. C., Oliver, B. R., Mudd, P. N., Kimbrough, C. L. and Miller, R. T. 2003, Fibrates induce peroxisomal and mitochondrial proliferation in cynomolgus monkeys without causing cell cycle alterations or oxidative stress. *The Toxicologist*, in press.

Reddy, J. K., Lalwani, N. D., Qureshi, S. A., Reddy, M. K. and Moehle, C. M. 1984, Induction of hepatic peroxisome proliferation in non-rodent species including primates. *American Journal of Pathology*, **114**, 171–183.

Roglans, N., Bellido, A., Rodriguez, C., Cabrero, A., Novell, F., Ros, E., Zambon, D. and Laguna, J. C. 2002, Fibrate treatment does not modify the expression of acyl coenzyme A oxidase in human liver. *Clinical Pharmacology and Therapeutics*, **72**, 692–701.

Romach, E. H., Shenk, J. L., Ott, R. J., Willson, T. M. and Miller, R. T. 2002, Hepatic effects of PPARδ are distinct from PPARα. *The Toxicologist*, **66**, 261.

Ross, C. R., Diezi-Chomety, F. and Roch-Ramel, F. 1975, Renal excretion of *N*(1-methylnicotinamide in the rat. *American Journal of Physiology*, **228**, 1641–1645.

Sanins, S. M., Nicholson, J. K., Elcombe, C. and Timbrell, J. A. 1990, Hepatotoxin-induced hypertaurinuria: a proton NMR study. *Archives of Toxicology*, **64**, 407–411.

Shibata, K. 1989, Fate of excess nicotinamide and nicotinic acid differs in rats. *Vitamins*, **119**, 892–895.

Shibata, K. and Matsuo, H. 1989a, Inhibition of *N*-methylnicotinamide oxidase activity by a large nicotinamide injection into rats. *Agricultural and Biological Chemistry*, **53**, 2031–2036.

Shibata, K. and Matsuo, H. 1989b, Inhibition of *N*-methylnicotinamide oxidase activity by a large amount of *N*-methylnicotinamide injected into rats. *Agricultural and Biological Chemistry*, **53**, 2393–2397.

Shibata, K., Kakehi, H. and Matsuo, H. 1990, Niacin catabolism in rodents. *Journal of Nutritional Science and Vitaminology*, **36**, 87–98.

Shibata, K., Kondo, T., Marugami, M. and Umezawa, C. 1996a, Increased conversion ratio of tryptophan to niacin by the administration of clofibrate, a hypolipidemic drug, to rats. *Bioscience, Biotechnology, and Biochemistry*, **60**, 1455–1459.

Shibata, K., Shimada, H. and Taguchi, H. 1996b, Fate of nicotinamide differs due to an intake of nicotinamide. *Bioscience, Biotechnology, and Biochemistry*, **60**, 1204–1206.

Shin, M., Mori, Y., Kimura, A., Fujita, Y., Yoshida, K., Sano, K. and Umezawa, C. 1996, NAD+ biosynthesis and metabolic fluxes of tryptophan in hepatocytes isolated from rats fed a chlofibrate-containing diet. *Biochemical Pharmacology*, **52**, 247–252.

Shin, M., Iwamoto, N., Yamashita, M., Sano, K. and Umezawa, C. 1998a, Pyridine nucleotide levels in liver of rats fed chlofibrate- or pyrazinamide-containing diets. *Biochemical Pharmacology*, **55**, 367–371.

Shin, M., Asada, S., Mizumori, N., Sano, K. and Umezawa, C. 1998b, Effect of thioridazine or chlorpromazine on increased hepatic NAD+ levels in rats fed clofibrate, a hypolipidaemic drug. *Journal of Pharmaceutical Pharmacology*, **50**, 431–436.

Shin, M., Nakakita, S., Hashimoto, C., Sano, K. and Umezawa, C. 1998c, NAD+ biosynthesis from tryptophan in the presence of nicotinic acid or vice versa by rat hepatocytes – effect of clofibrate-feeding. *International Journal for Vitamin and Nutrition Research*, **68**, 104–108.

Shin, M., Ohnishi, M., Iguchi, S., Sano, K. and Umezawa, C. 1999a, Peroxisome-proliferator regulates key enzymes of the tryptophan-NAD+ pathway. *Toxicology and Applied Pharmacology*, **158**, 71–80.

Shin, M., Sano, K. and Umezawa, C. 1999b, Effects of peroxisome-proliferators on the TRP-NAD pathway. *Advances in Experimental Medicine and Biology*, **467**, 333–340.

Tamulevicius, P. and Streffer, C. 1984, *N*-Methylnicotinamide as a possible prognostic indicator of recovery from leukaemia in patients treated with total-body irradiation and bone marrow transplants. *Strahlentherapie*, **160**, 249–254.

Tanabe, A., Egashira, Y., Fukuoka, S., Shibata, K. and Sanada, H. 2002, Expression of rat hepatic 2-amino-3-carboxymuconate-6-semialdehyde decarboxylase is affected by a high protein diet and by streptozotocin-induced diabetes. *Journal of Nutrition*, **132**, 1153–1159.

Tucker, M. J. and Orton, T. C. 1995, *Comparative Toxicology of Hypolipidaemic Fibrates* (London: Taylor & Francis).

Wold, S., Antti, H., Lindgren, F. and Ohman, J. 1998, Orthogonal signal correction of near-infrared spectra. *Chemometrics and Intelligent Laboratory Systems*, **44**, 175–185.

WOLF, H. 1974, Studies on tryptophan metabolism in man: the effect of hormones and vitamin B6 on urinary excretion of metabolites of the kynurenine pathway. *Scandinavian Journal of Clinical and Laboratory Investigation Supplementum*, **136**, 1–186.

YUYAMA, S. and SUZUKI, T. 1985, Isolation and identification of *N*-methylnicotinic acid (Trigonelline) from rat urine. *Journal of Nutritional Science and Vitaminology*, **31**, 157–167.